Intestinal Farnesoid X Receptor Controls Transintestinal Cholesterol Excretion in Mice

Boer, de, Jan Freark; Schonewille, Marleen; Boesjes, Marije; Wolters, Henk; Bloks, Vincent W; Bos, Trijnie; van Dijk, Theo H; Jurdzinski, Angelika; Boverhof, Renze; Wolters, Justina C

Published in:
Gastroenterology

DOI:
10.1053/j.gastro.2016.12.037

Publication date:
2017

Accepted Manuscript

Intestinal Farnesoid X Receptor Controls Transintestinal Cholesterol Excretion in Mice

Jan Freark de Boer, Marleen Schonewille, Marije Boesjes, Henk Wolters, Vincent W. Bloks, Trijnie Bos, Theo H. van Dijk, Angelika Jurdzinski, Renze Boverhof, Justina C. Wolters, Jan A. Kuivenhoven, Jan M. van Deursen, Ronald P.J. Oude Elferink, Antonio Moschetta, Claus Kremoser, Henkjan J. Verkade, Folkert Kuipers, Albert K. Groen

PII: S0016-5085(17)30005-7
DOI: 10.1053/j.gastro.2016.12.037
Reference: YGAST 60898

To appear in: *Gastroenterology*
Accepted Date: 23 December 2016

Please cite this article as: de Boer JF, Schonewille M, Boesjes M, Wolters H, Bloks VW, Bos T, van Dijk TH, Jurdzinski A, Boverhof R, Wolters JC, Kuivenhoven JA, van Deursen JM, Oude Elferink RPJ, Moschetta A, Kremoser C, Verkade HJ, Kuipers F, Groen AK, Intestinal Farnesoid X Receptor Controls Transintestinal Cholesterol Excretion in Mice, *Gastroenterology* (2017), doi: 10.1053/j.gastro.2016.12.037.

TITLE

Intestinal Farnesoid X Receptor Controls Transintestinal Cholesterol Excretion in Mice

SHORT TITLE

Bile salts control cholesterol turnover

AUTHORS

Jan Freark de Boer[1,*], Marleen Schonewille[1,*], Marije Boesjes[1,*], Henk Wolters[1], Vincent W. Bloks[1], Trijnie Bos[2], Theo H. van Dijk[2], Angelika Jurdzinski[1], Renze Boverhof[2], Justina C. Wolters[1], Jan A. Kuivenhoven[1], Jan M. van Deursen[3], Ronald P.J. Oude Elferink[4], Antonio Moschetta[5], Claus Kremoser[6],Henkjan J. Verkade[1], Folkert Kuipers[1,2], Albert K. Groen[1,2]

Conflicts of interest:

Dr. Claus Kremoser is CEO of Phenex Pharmaceuticals AG, Heidelberg, Germany.

The other authors have no conflicts of interest to declare.

AFFLIATIONS

Departments of [1]Pediatrics and [2]Laboratory Medicine, University of Groningen, University Medical Center Groningen, Groningen, The Netherlands.

[3]Departments of Pediatric and Adolescent Medicine, and Biochemistry and Molecular Biology, Mayo Clinic College of Medicine, Rochester, MN, USA

[4]Tytgat Institute for Liver and Intestinal Research and Department of Hepatology & Gastroenterology, Academic Medical Center, University of Amsterdam, Amsterdam, The Netherlands.

[5]Department of Interdisciplinary Medicine, University of Bari and IRCCS Istituto Tumori "Giovanni Paolo II", Bari, Italy.

[6]Phenex Pharmaceuticals AG, Heidelberg, Germany

[*] These authors contributed equally

GRANT SUPPORT

Supported within the framework of Top Institute Pharma, The Netherlands, project T2-110 and in part by European Union grant FP7- HEALTH n°305707

Abbreviations used in this paper:

ABCG5/G8, ATP binding cassette subfamily G member 5/8; ABCB1A/B, ATP-Binding Cassette, Sub-Family B (MDR/TAP) Member 1 A/B; CA, cholic acid; CDCA, chenodeoxycholic acid; CTRL, control; CYP7A1, cytochrome P450 family 7 subfamily A member 1; CYP8B1, cytochrome P450 family 8 subfamily B member 1; DCA, deoxycholic acid; EZE, ezetimibe; Fa, fractional absorption; FGF15/19, fibroblast growth factor 15/19; FNS, fecal neutral sterols; FXR (NR1H4), farnesoid X receptor; IFXR KO, intestine-specific

FXR KO; IFXR TG, intestine-specific FXR transgenic; HDCA, hyodeoxycholic acid; HMGCR, 3-hydroxy-3-methylglutaryl-CoA reductase; HPLC, high-performance liquid chromatography; KEGG, kyoto encyclopedia of genes and genomes; LCA, lithocholic acid; LDL, low-density lipoprotein; LXR, liver X receptor; MCA, muricholic acid; PX, PX20606; SHP (NR0B2), small heterodimer partner; SR-BI, scavenger receptor class B, member 1; TICE, transintestinal cholesterol excretion; UDCA, ursodeoxycholic acid; WT, wild-type;

CORRESPONDENCE

J.F. de Boer

email: j.f.de.boer@umcg.nl

Transcript profiling:

http://www.ncbi.nlm.nih.gov/geo/query/acc.cgi?token=irsrayeohfcntqx&acc=GSE74101

AUTHOR CONTRIBUTIONS

Jan Freark de Boer: study concept and design, acquisition of data, analysis and interpretation of data, statistical analysis, drafting of the manuscript

Marleen Schonewille: study concept and design, acquisition of data, analysis and interpretation of data, statistical analysis, drafting of the manuscript

Marije Boesjes: study concept and design, acquisition of data, analysis and interpretation of data, statistical analysis, drafting of the manuscript

Henk Wolters: technical support, acquisition of data

Vincent W. Bloks: technical support, manuscript revision

Trijnie Bos: technical support, acquisition of data

Theo H. van Dijk: technical support, acquisition of data

Angelika Jurdzinksi: technical support, acquisition of data

Renze Boverhof: technical support, acquisition of data

Justina C. Wolters: acquisition of data, analysis and interpretation of data

Jan A. Kuivenhoven: analysis and interpretation of data, manuscript revision

Jan van Deursen: Generation iFXR mice, manuscript revision

Ronald P.J. Oude Elferink: Study concept and design, manuscript revision

Antonio Moschetta: Providing critical reagents, manuscript revision

Claus Kremoser: material support, manuscript revision

Henkjan J. Verkade: study concept and design, manuscript revision

Folkert Kuipers: study concept and design, manuscript revision

Albert K. Groen: study concept and design, manuscript revision, study supervision

Abstract:

Background & Aims: The role of the intestine in the maintenance of cholesterol homeostasis is increasingly recognized. Fecal excretion of cholesterol is the last step in the atheroprotective reverse cholesterol transport pathway, to which biliary and transintestinal cholesterol excretion (TICE) contribute. The mechanisms controlling the flux of cholesterol through the TICE pathway are, however, poorly understood. We aimed to identify mechanisms that regulate and stimulate TICE.

Methods: We performed studies with C57Bl/6J mice, as well as mice with intestine-specific knockout of the farnesoid X receptor (FXR), mice that express an *FXR* transgene specifically in the intestine, and ABCG8-knockout mice. Mice were fed a control diet or a diet supplemented with the FXR agonist PX20606, with or without the cholesterol absorption inhibitor ezetimibe. Some mice with intestine-specific knockout of FXR were given daily injections of fibroblast growth factor (FGF)19. To determine fractional cholesterol absorption, mice were given intravenous injections of cholesterol-D5 and oral cholesterol-D7. Mice were given ^{13}C-acetate in drinking water for measurement of cholesterol synthesis. Bile cannulations were performed and biliary cholesterol secretion rates were assessed. In a separate set of experiments, bile ducts of male Wistar rats were exteriorized, allowing replacement of endogenous bile by a model bile.

Results: In mice, we found TICE to be regulated by intestinal FXR, via induction of its target gene *Fgf15* (in mouse; *FGF19* in rat and human). Stimulation of this pathway caused mice to excrete up to 60% of their total cholesterol content each day. PX20606 and FGF19 each increased the ratio of muricholate:cholate in bile, inducing a more hydrophilic bile salt pool. The altered bile salt pool stimulated robust secretion of cholesterol into the intestinal lumen via the sterol-exporting heterodimer ATP binding cassette subfamily G member 5/8 (ABCG5/G8). Of note, the increase in TICE induced by PX20206 was independent of changes in cholesterol absorption.

Conclusions: Hydrophilicity of the bile salt pool, controlled by FXR and FGF15/19, is an important determinant of cholesterol removal via TICE. Strategies that alter bile salt pool composition might be developed for prevention of cardiovascular disease.

KEY WORDS: RCT; TICE; metabolism; ABCG5/G8

INTRODUCTION

The role of the liver in the maintenance of cholesterol homeostasis is well established. By serving as a major site of cholesterol synthesis, lipoprotein production and uptake, and catabolism of cholesterol through bile salt synthesis as well as by secretion of vast amounts of sterols into the bile, the liver acts as chief regulator of cholesterol metabolism.[1] More recently, it has become clear that the intestine also plays an eminent role in the control of the body's cholesterol balance by mechanisms beyond control of cholesterol absorption.[2,3] We[4] and others[5,6] recently showed that, in addition to removal from the body via biliary sterol secretion, cholesterol can also be transported directly from blood into the intestinal lumen preparatory to its excretion with the feces. This pathway is now known as transintestinal cholesterol excretion or TICE.[7,8] Under standard laboratory conditions, this pathway accounts for approximately 30% of fecal neutral sterol (i.e., cholesterol and its bacterial derivatives) output in mice. Despite its evident importance in control of cholesterol homeostasis, the molecular mechanisms and control of TICE have remained largely elusive. We have demonstrated that cholesterol excretion via the TICE pathway can be stimulated by liver X receptor (LXR)-agonism and by plant sterols, indicating a regulatory role for the sterol transporting heterodimer ATP binding cassette subfamily G member 5/8 (ABCG5/G8).[4,9] In addition, Le May et al. suggested a role for the multidrug transporter ATP-binding cassette, sub-family B (MDR/TAP), Member 1 (ABCB1) and proposed regulatory activities by proprotein convertase subtilisin/kexin type 9 (PCSK9).[5] More recently, flavin monooxygenase 3 (FMO3) has been implicated in TICE regulation.[10]

Cholesterol serves as substrate for the production of steroid hormones but is also indispensable for bile salt synthesis in the liver. Following biliary secretion, bile salts enter the intestinal lumen where their presence is essential for cholesterol absorption to occur.[11] A considerable number of different bile salt species is normally present within a single individual. The physical-chemical characteristics of bile salts influence their lipid-solubilizing properties as well as their signaling abilities (see Kuipers et al.[12], Li and

Chiang[13] for recent reviews), thereby permitting metabolic control via regulation of the bile salt pool composition. The farnesoid X receptor (NR1H4/FXR) is the central actor controlling bile salt synthesis and is expressed mainly in the liver and small intestine.[14-16] Intestinal FXR has been shown to play a pivotal role in regulating hepatic bile salt synthesis and bile salt pool composition through promoting the production of fibroblast growth factor 15 (FGF15; FGF19 in humans) that inhibits bile salt synthesis in the liver.[17]

In the present study, we reveal that agonism of intestinal FXR greatly enhances the flux of cholesterol through the TICE pathway in a manner that largely depends on ABCG5/G8 function in the intestine. The composition of the bile salt pool conceivably impacts the rate of cholesterol removal from the body via TICE. Our data strongly suggests that a high proportion of hydrophilic bile salts stimulates this route via activation of ABCG5/G8 in the intestine. Importantly, the magnitude of the increase in TICE induced by FXR agonism remained similar under conditions in which cholesterol absorption was blocked by ezetimibe. This demonstrates that decreased cholesterol absorption is not the mechanism by which fecal neutral sterol excretion is stimulated upon FXR activation but that the flux of cholesterol into the intestinal lumen is actually enhanced.

MATERIALS AND METHODS

Animal experiments

Male age-matched wild-type (WT) C57Bl/6J mice, intestine-specific FXR knock-out (iFXR KO)[18] and their WT littermates, intestine-specific FXR-transgenic mice (iFXR TG; see supplemental materials and methods) and their non-transgenic littermates (FXR KO)[19] as well as ABCG8 knock-out (ABCG8 KO) mice and their WT littermates[20] were housed in a light (12:12)- and temperature-controlled (21°C) facility and received standard rodent diet (RMH-B, Hope Farms, Woerden, The Netherlands) *ad libitum*. When stated, mice received 10 mg/kg/day PX20606 (PX) (Phenex Pharmaceuticals, AG, Heidelberg, Germany)[21,22], 0.005% (w/w) ezetimibe (Ezetrol; Pharmacy UMCG, Groningen, The Netherlands), or both compounds mixed into their diet. Additionally, ABCG8 KO mice were injected with 1 x 10^{11} particles/mouse of an Abcg8-encoding adenovirus (AdABCG8) or control virus (AdNull) and experiments were performed between day 3 and day 5 after administration. Furthermore, iFXR KO mice were injected (i.p) with 1 mg/kg/day FGF19 (generous gift of dr. J. Nguyen, NGM Biopharmaceuticals San Francisco, USA) for 8 consecutive days when indicated. Experiments were conducted in conformity with the law on the welfare of laboratory animals and experimental procedures were approved by the responsible ethics committees.

Experimental procedures

To determine fractional cholesterol absorption, mice received an intravenous dose of 0.3 mg cholesterol-D5 (Medical Isotopes, Inc, Pelham, NH, USA) dissolved in Intralipid (20%, Fresenius Kabi, Den Bosch, The Netherlands) and an oral dose of 0.6 mg cholesterol-D7 (Cambridge Isotope Laboratories, Inc, Andover, MA, USA) in medium-chain triglyceride oil 10 days prior to the end of the experiment.

Mice received ^{13}C-acetate via the drinking water 3 days prior to the end of the experiment in order to determine cholesterol synthesis. At the end of the experiment, mice were anesthetized and bile cannulation was performed.[23] In a separate series of experiments male Wistar rats (Sulzfeld, Germany) were surgically equipped with permanent cannulas in their bile duct and duodenum.[24] The outlets of the cannulas were fixed on the head of the animals. After surgery, the animals were allowed to recover for 5 days. During this period, the cannulas from the bile duct and duodenum were connected to each other on the head of the animals, essentially restoring the enterohepatic circulation via an extended bile duct. After having obtained feces for determination of fecal neutral sterol (FNS) excretion, the enterohepatic circulation was interrupted and all bile of the rats was quantitatively collected in a tube located outside the cage. From the moment of interruption, model bile was infused into the intestinal cannula. All animals received identical model bile composed of 15 mM taurocholic acid and 2.5 mM phosphatidylcholine at a rate of 1.2 mL/hour. PX20606 (10 mg/kg/day) was provided via the diet when indicated, starting two weeks before interruption of the enterohepatic circulation.

Analytical procedures

Plasma triglycerides, total cholesterol and free cholesterol were determined using commercially available kits (Roche Diagnostics, Mannheim, Germany and DiaSys Diagnostic Systems, Holzheim, Germany) or using gas chromatography after trimethylsilylation as described below. Biliary cholesterol was quantified by gas chromatography as described below for measurement of fecal neutral sterols.[25] Biliary and fecal bile salt composition were quantified using capillary gas chromatography as described.[26] The hydrophobicity index of the bile salt pool was calculated according to Heuman.[27] Fecal cholesterol and its derivatives were trimethylsilylated with pyridine, N,O-Bis (trimethylsilyl) trifluoroacetamide and trimethylchlorosilane and measured with gas chromatography. Cholesterol label enrichment was determined by capillary gas chromatography on a Agilent gas chromatograph (7890A; Amstelveen, The Netherlands) connected to a Agilent mass spectrometer (5975C). Cholesterol was derivatized with N,O-

Bis (trimethylsilyl) trifluoroacetamide containing 1% trimethylchlorosilane. Isotope ratios were determined in the selected ion monitoring mode on m/z 458 (M0) to 465 (M7). Cholesterol absorption and synthesis were calculated as described elsewhere.[4,9,28] TICE was calculated by subtracting the contribution of dietary and biliary cholesterol to fecal neutral sterols after correcting for absorption according to the formula TICE=FNS-(($Chol_{diet}$+$Chol_{bile}$)*(1-Fa)), where FNS is fecal neutral sterols and Fa is fractional cholesterol absorption.[28]

RNA isolation and measurement of mRNA levels by quantitative real-time PCR

Total RNA was isolated using TRI-Reagent (Sigma, St. Louis, MO, USA). cDNA was produced using Moloney-Murine Leukemia Virus reverse transcriptase (Life Technologies, Bleiswijk, The Netherlands). Real-time qPCR analysis was performed on a 7900HT Fast Real-Time PCR system (Applied Biosystems, Darmstadt, Germany) and gene expression levels were normalized to 36B4.

Western blotting for ABCG5 protein expression

Intestinal brush border membranes were isolated as described by Schmitz et al.[29] Equal amounts of brush border membranes (10 µg protein) for detection of ABCG5 were electrophoresed and blotted on Hybond ECL membranes (Amersham, Little Chalfont, UK). Membranes were incubated with anti-ABCG5 primary antibody.[30] Immune complexes were visualized using horseradish peroxidase-conjugated goat anti-rabbit (DAKO, Heverlee, Belgium) and SuperSignal West Dura substrate (ThermoScientific, Rockford, IL, USA).

Statistics

Statistical analysis was performed by Kruskal-Wallis H test followed by Conover post-hoc comparisons using Brightstat.[31] Correlations were analyzed by Spearman's correlation using Graphpad Prism. Differences were considered statistically significant when $p<0.05$.

RESULTS

Pharmacological activation of intestinal FXR markedly enhances fecal neutral sterol excretion in mice

To delineate the role of bile salts in control of body cholesterol fluxes, we chose to modify bile salt synthesis and pool composition via modulation of the activity of the bile salt-activated nuclear receptor FXR. C57BL/6J mice were treated with the FXR agonist PX20606 (PX) for two weeks. In line with data obtained in hyperlipidemic mice and monkeys[22], the compound was well-tolerated and had no effect on body weight or food intake (data not shown). PX treatment decreased plasma cholesterol and triglycerides (Figure 1A,B) but increased hepatic levels of these lipids (Figure S1A,B). In keeping with the regulatory role of FXR in bile salt synthesis, PX treatment decreased fecal bile salt output (Figure 1C) which, in steady state conditions, reflects hepatic bile salt production. Furthermore, PX treatment strongly increased fecal neutral sterol (FNS) excretion (Figure 1D). Stably labeled cholesterol tracers were used to investigate the effects of PX on cholesterol absorption. Fractional cholesterol absorption was reduced in mice treated with the FXR agonist (Figure 1E). To explore whether decreased cholesterol absorption contributed to the augmented cholesterol removal with the feces, ezetimibe was added to the treatment regimen of the mice. Ezetimibe is a potent inhibitor of cholesterol absorption (Figure 1E) and therefore enabled us to study the absorption-independent effects of PX. Combination treatment of ezetimibe and PX led to an additional decrease in plasma lipid levels (Figure 1A,B and S1C,D). Interestingly, ezetimibe given in combination with PX led to a FNS excretion that was at least equal to the sum of both individual treatments, generating a very high rate at which cholesterol was removed from the body (Figure 1D). Of note, about 8 days of PX treatment were needed to reach maximal effects on FNS excretion, while the maximal effect of ezetimibe was established much earlier (Figures 1F and S2). Bile flow was doubled in PX-treated mice and this was not affected by co-treatment with ezetimibe (Figure 2A). Although the concentration of bile salts in the bile was lower in response to treatment with

PX, biliary bile salt secretion was not altered due to the increased bile flow (Figure 2B). Treatment of mice with the FXR agonist caused an increase of biliary cholesterol secretion while ezetimibe hardly impacted this flux (Figure 2C). When FNS excretion, dietary cholesterol intake, biliary cholesterol secretion and fractional cholesterol absorption are known, TICE can be calculated. Cholesterol removal via TICE was 142 µmol/day/100g body weight (>17-fold) higher in PX-treated mice compared to untreated controls (Figure 2D). PX treatment in combination with ezetimibe led to an increase of TICE with 238 µmol/day/100g compared to mice receiving ezetimibe only, indicating that PX indeed operates via a different mechanism as ezetimibe. Analysis of cholesterol tracer kinetics revealed that PX stimulated elimination of intravenously injected cholesterol-D_5 from the plasma compartment (Figure 2E). Notably, analysis of tracer within the feces revealed that PX-treated mice had excreted 68% of i.v. injected tracer into the feces at 72 h after injection whereas this was only 7.8% in control mice (Figure 2F), indicating that cholesterol extracted from the plasma compartment indeed ended up in feces. Treatment with PX and ezetimibe caused the strongest excretion of tracer (85% of the injected dose).

To verify the selectivity and specificity of PX, we also performed experiments in whole-body FXR knock-out mice. PX did not impact FNS excretion (Figure S3) in these mice nor any of the other parameters studied, confirming that the observed effects were indeed mediated through FXR.

The role of intestinal FXR in control of cholesterol fluxes

PX has been shown to activate both hepatic and intestinal FXR.[22] To disentangle the effects of hepatic and intestinal FXR, we performed experiments in intestine-specific FXR (iFXR) KO mice. Interestingly, the PX-induced changes in cholesterol fluxes were almost completely abrogated in these mice; only marginal inductions of FNS excretion (Figure 3A) and TICE (Figure 3B) were observed and, in contrast to WT mice, fractional cholesterol absorption was not affected by PX treatment in the iFXR KO mice (Figure

3C). This indicates that intestinal FXR plays a major role in the control of whole-body cholesterol turnover. To more clearly delineate the role of intestinal FXR in control of cholesterol fluxes, we rescued intestinal FXR expression in a total body FXR KO background. Transgenic intestine-specific FXR expressing mice (iFXR TG) were generated using the murine FXR gene under control of the villin promoter (Figure S4). No overt phenotypic differences between FXR KO and iFXR TG mice were noticed when kept under standard laboratory conditions. Treatment of iFXR TG mice with PX did not reduce plasma cholesterol and triglyceride levels (Figures 4A,B). This suggests that hepatic FXR rather than intestinal FXR mediates the reduction of plasma lipids in response to PX. The compound also did not affect liver weight and biliary cholesterol secretion (data not shown). Reinstitution of intestinal FXR expression in FXR KO mice did, however, restore the PX-induced increase in FNS excretion and TICE substantially (Figure 4C,D). Together, these data highlight the critical role of intestinal FXR in the stimulation of cholesterol removal via TICE upon treatment with PX. Furthermore, fractional cholesterol absorption (Figure 4E) and fecal bile salt output (Figure 4F) were decreased in response to PX treatment in iFXR TG mice.

Transport of cholesterol from enterocytes into the intestinal lumen

Next, we addressed the mechanism via which cholesterol is secreted into the intestinal lumen. Being an established cholesterol transporter present at the luminal side of enterocytes, the ABCG5/G8 heterodimer is a potential mediator of the TICE pathway. PX increased *Abcg5/g8* expression in the liver but had no effect in the small intestine whereas ezetimibe slightly increased hepatic expression of *Abcg5*/*g8* but decreased the expression in the proximal small intestine (Figure 5A). The effect on intestinal gene expression was mirrored at protein level (Figure 5A, right panel). Since expression levels of genes/proteins do not necessarily reflect activity, we investigated whether the heterodimer is

involved in stimulation of FNS excretion and TICE by PX using ABCG8 KO mice. Single ABCG8 knock-out mice phenocopy ABCG5/G8 double knock-outs because the proteins need to dimerize to allow trafficking of the transporter to the apical membrane of hepatocytes and enterocytes.[32] We challenged ABCG8 KO mice and WT littermates with PX either or not in combination with ezetimibe and assessed the effects on body cholesterol fluxes. Severely blunted inductions of FNS excretion (Figure 5B, left panel) and TICE (Figure 5C, left panel) in response to treatment with PX or PX/ezetimibe clearly demonstrate that ABCG5/G8 is mediating the vast majority of cholesterol that is secreted via the TICE pathway under these stimulated conditions. In conformity with the established role of ABCG5/G8 regarding secretion of hepatic cholesterol into the bile, the PX-induced increase in biliary cholesterol secretion was absent in ABCG8 KO mice (Figure 5D, left panel). Interestingly, despite the blunted induction of FNS excretion, PX and dual treatment did considerably impact plasma cholesterol levels (Figure 5E, left panel), suggesting that the decrease of plasma cholesterol induced by PX is not merely the consequence of increased intestinal excretion. ABCG5/G8 is expressed in the liver and intestine. Therefore, reintroduction of ABCG8 in the liver by adenoviral transfection in ABCG8 KO mice allows the investigation of the effects of ABCG5/G8 deficiency specifically in the intestine. Using this model, we investigated the impact of intestinal ABCG5/G8 on cholesterol fluxes in response to PX and PX/ezetimibe. Adenoviral rescue of hepatic ABCG8 expression in ABCG8 KO mice had very little impact on FNS excretion, TICE and plasma cholesterol levels despite a restoration of biliary cholesterol secretion (Figure 5B-E, right panels). These data pinpoint intestinal ABCG5/G8 as the transporter mediating most of the cholesterol excretion in mice treated with either PX alone or PX/ezetimibe.

The mechanism by which intestinal FXR activation and ezetimibe induce TICE

FXR is expressed throughout the small intestine but is considered to act under physiological conditions mainly via bile salt signaling in the distal part of the ileum. Yet, PX may activate FXR all along the small intestine and thereby stimulate TICE at the site where it is most active, i.e., in the proximal small intestine.[7] To analyze which genes/pathways were targeted by PX, we performed microarray analysis in the proximal intestine at an FDR of 5%. Figure S5A shows the results for Kyoto encyclopedia of genes and genomes (KEGG) pathway analysis; genes involved in Parkinson's disease, Huntington disease and oxidative phosphorylation came up in the proximal part of the small intestine. KEGG pathway analysis of the array data derived from the distal small intestine gave a very different pattern (Figure S5B) with nitrogen metabolism being the most regulated pathway. In contrast, cholesterol synthesis was the most prominently regulated pathway in the liver, indicating that the mobilized cholesterol was replenished at least in part by the *de novo* synthesis in the liver (Figure S5C).

Validation by PCR confirmed the results of the KEGG pathway analysis in liver pointing towards increased cholesterol synthesis, and showed the downregulated expression of sterol 12-alpha-hydroxylase (*Cyp8b1*) and cholesterol 7-alpha-hydroxylase (*Cyp7a1*) as a consequence of FXR agonism (Figure S5D). Application of mass isotopomer distribution analysis after administration of ^{13}C-acetate indeed demonstrated augmented cholesterol synthesis in response to PX treatment, which was further induced when mice were co-treated with ezetimibe (Figure 6A). In the small intestine, FXR activation induced the expected upregulation of *Fgf15* (Figure S6A) which is thought to mediate most of the physiological relevant effects of intestinal FXR on the liver. When FGF15 mediates the effects of PX on FNS excretion and TICE, treatment with FGF15/19 should at least partially rescue the lack of effect of PX in iFXR KO mice. Therefore, PX-treated iFXR KO mice were challenged for eight days with the human orthologue FGF19 and FNS output was compared to mice only receiving PX. As evident from the data shown in Figure 6B, FGF19 rescued FNS excretion thereby identifying FGF15/19 as a crucial factor mediating increased FNS loss in response to FXR agonism by PX. Next, we explored the mechanistic basis

underlying the restoration of PX-induced stimulation of FNS excretion by FGF15/19. Both PX and FGF15 control bile salt synthesis but via differential effects on expression of *Cyp7a1* and *Cyp8b1* (Figures 6C and S6B), leading to an altered balance between the cholate and chenodeoxycholate/muricholate synthesis pathways. We therefore determined bile salt species composition in the iFXR KO mice treated with PX and/or FGF19 (Figure 6D). Interestingly, FGF19 seemed to be required for the shift of the balance towards the relatively hydrophilic muricholates instead of the more hydrophobic cholate and deoxycholate. This interesting observation let us to study the relationship between the hydrophobicity index (HI) of biliary bile salts, calculated according to Heuman[27], and FNS excretion. A clear negative correlation emerged (Figure 6E), suggesting that hydrophilic bile salts stimulate FNS excretion via the TICE pathway. Of note, the hydrophilicity of the fecal bile salt pool changed steadily over a period of 8 days during PX treatment (Figure S7), in line with the gradual increase in FNS (see Figure 1F). In ABCG8 KO mice the changes in the bile salt pool composition were similar to those observed in WT mice (Figure 6F). This translated into only minute effects on FNS excretion and TICE (Figure 5B,C), suggesting a functional interaction of hydrophilic bile salts with the ABCG5/G8 transporter in the intestine.

If hydrophilic bile salts would indeed be responsible for the increased FNS excretion as a result of increased TICE, PX would fail to stimulate FNS excretion in bile-diverted animals. However, cholesterol excretion via TICE requires the presence of acceptor particles (i.e., bile salt and phospholipid micelles) in the intestine.[7] Therefore, we used rats with exteriorized bile ducts[24] that were treated with either vehicle or PX. Small bile samples taken from the still intact enterohepatic circulation revealed that PX treatment in rats also led to an increase in the relative abundance of hydrophilic muricholates (Figure 7A). Analysis of the feces obtained at this stage revealed that PX indeed stimulated FNS excretion in these animals (Figure 7B). Next, the enterohepatic circulation was interrupted and long-term bile diversion combined with model bile infusion was performed under non-anaesthetized conditions. All animals received identical model bile composed of taurocholate and phosphatidylcholine, ensuring

identical bile salt actions in the intestine. If PX would mediate its effects by affecting the bile salt pool composition, the effects would be lost after interruption of the enterohepatic circulation and start of the model bile infusion. Indeed, the PX-induced stimulation of FNS excretion was completely abrogated when the enterohepatic circulation was interrupted and the rats were receiving the identical model bile (Figure 7B). Of note, gene expression analysis confirmed upregulation of *Fgf19* in the ileum as well as enhanced hepatic expression of small heterodimer partner (*Nr0b2/Shp*) along with downregulation of *Cyp7a1* and *Cyp8b1* in the PX-treated rats, indicating that the FXR agonist was functionally active in the bile-diverted animals (Figure 7C).

DISCUSSION

In this study we demonstrate that the intestine itself has the capability to facilitate elimination enormous amounts of cholesterol from the body via the TICE pathway. The large capacity of TICE that became evident from the current studies highlights the potential of the intestine as a target for future cholesterol-lowering therapies. The induction of TICE in response to FXR activation appears to be mediated by hydrophilic bile salts. The fact that the magnitude of induction of FNS excretion and TICE by PX was virtually identical under conditions in which cholesterol absorption was blocked strongly suggests that the presence of bile salts in the intestinal lumen is not only a prerequisite for uptake of dietary and biliary cholesterol by the enterocytes but, additionally, an important determinant of excretion of plasma-derived cholesterol by the enterocytes into the intestinal lumen and hence of whole-body cholesterol turnover.

The large capacity of the intestine to remove plasma-derived cholesterol becomes evident from a comparison between the measured values of TICE with estimates of the total amount of cholesterol that is present within the mouse body. The total cholesterol pool in mice has been estimated to be about 50 mg.[33] PX/ezetimibe treatment increased FNS excretion to about 30 mg per 24 hours, implying that an amount equal to ~60% of the entire body pool is excreted each day. Since the sum of biliary secretion and dietary intake of cholesterol in our experimental set up amounted to maximally 5 mg/day, TICE has to account for at least 25 mg/day (i.e., 80% of total cholesterol disposal) under these conditions. Earlier studies from our laboratories indicated that the sterol transporting heterodimer ABCG5/G8 might play a role in the TICE pathway.[4,9,34] Our present results suggest that the physical chemical properties of luminal bile salts impact the activity of ABCG5/G8 at the intestinal brush border membrane and thereby take part in the control of TICE, at least under the TICE-stimulating conditions employed in this study. Note that, in absence of ABCG5/G8 activity, dual treatment with PX and ezetimibe still activated TICE up

to 33 µmol/day/100g (15% of wild-type values), suggesting that there is another transport system present that can partly compensate for ABCG5/G8. In support of this, Wang et al. showed recently that feeding ABCG5/G8 double knock-out mice with ursodeoxycholate stimulated FNS excretion considerably.[35] As suggested by Le May et al.[5], the multidrug resistance transporter ABCB1 may be responsible for the ABCG5/G8-independent TICE flux or a part thereof. We did not detect increased intestinal expression of the *Abcb1a* and *b* genes under any of the stimulated conditions (data not shown). However, we also did not observe increased expression of ABCG5/G8, even under very high flux conditions. This indicates that this heterodimer has a very high intrinsic transport capacity.

Whereas the synthetic FXR agonist obeticholic acid (OCA, INT-747, 6-ECDCA) closely resembles chenodeoxycholic acid, PX20606 is structurally related to GW4064.[21] PX was shown previously to potently decrease plasma cholesterol levels and progression of atherosclerosis in cholesteryl ester transfer protein (CETP)-transgenic/low-density lipoprotein (LDL)-receptor knock-out mice.[22] At first sight, our results indicate that mobilization of cholesterol, driven by increased TICE, may explain the cholesterol-lowering effect in plasma. Indeed, plasma cholesterol was also reduced in PX-treated wild-type mice in our study (Figure 1A). However, when increased TICE would underlie the reduction of plasma cholesterol levels, the same phenomenon should have been observed in the iFXR-TG mice on a FXR-KO background. Yet, despite a considerable rescue of TICE activity in these mice there was very little effect on plasma cholesterol. It is therefore most conceivable that reduction of plasma cholesterol upon PX treatment in mice that do express hepatic FXR is due to suppressed transcription of apolipoprotein A-I[36] and enhanced expression of scavenger receptor class B-I (SCARB1/SR-BI) upon FXR activation, as reported previously by others.[37] In keeping with this hypothesis, we found upregulation of hepatic SR-BI mRNA as well as protein (data not shown). Thus, *de novo* cholesterol synthesis by the liver, as supported by a profound upregulation of *Hmcgr* expression and direct quantification of cholesterol synthesis using mass isotopomer distribution analysis, apparently compensates for the increased loss of cholesterol by

TICE-mediated sterol excretion. On the other hand, inspection of the effect of PX on global gene expression in the proximal small intestine (Figure S5A) revealed that cholesterol synthesis or transport were not among the most regulated pathways in KEGG analyses, suggesting that the stimulatory effect of PX on cholesterol trafficking was not determined by intestinal cholesterol production.

Although the PX-induced stimulation of FNS excretion and TICE was substantial in iFXR-TG mice it was still considerably less when compared to wild-type mice, suggesting a role for hepatic FXR in controlling the rate of TICE. It was recently reported that FXR increases the hepatic response to FGF15/19, via stimulation of fibroblast growth factor receptor 4 (FGFR4) stability by the FXR target ß-klotho.[38] This mechanism could potentially explain the different FNS excretion between PX-treated wild-type and iFXR-TG mice, which lack expression of FXR in the liver and therefore are likely less responsive to FGF15/19. Yet, administration of FGF19 to iFXR KO mice fully rescued the effect of PX on FNS and TICE, which might be due to supraphysiological plasma levels after FGF19 treatment. Indeed, FGF19 alone was sufficient to induce cholesterol mobilization. Studies from the group of Kliewer and Mangelsdorf demonstrated direct effects of this intestinal hormone on glucose, lipid and bile salt metabolism.[39,40] However, intestinal cholesterol trafficking was not addressed. The role of FGF15/19 in regulation of bile salt synthesis has been described in detail[40] and these results are confirmed in the present study. Treatment with PX had a strong impact on the relative contribution of the cholate and chenodeoxycholate/muricholate pathways to overall bile salt synthesis in wild-type mice. Consequently, the ratio of muricholates to cholate in bile increased considerably. This effect of PX on bile salt species distribution was absent in iFXR KO mice, but was regained when FGF19 was co-administered to these animals. Surprisingly, although treatment with FGF19 alone did not appear to have major impact on CYP8B1 mRNA and protein expression, it did induce a muricholate-dominated bile salt pool. Note that mRNA and protein levels reflect expression of CYP8B1 at one particular moment during the circadian cycle and may therefore not be an accurate measure of activity over the day. Bile salt pool composition

on the other hand provides a physiologically relevant indication of the relative activities of the cholate and chenodeoxycholate synthesis pathways over time. We have shown in an earlier study that ABCG5/G8-mediated cholesterol efflux in cultured cells is stimulated more strongly by the hydrophilic bile salt ursodeoxycholate compared to the more hydrophobic cholate.[41] This difference between bile salt species now also appears to be of great physiological relevance *in vivo*. As a matter of fact, our data suggest that bile salt species distribution actually underlies the stimulatory effect of PX on FNS excretion and TICE (Figure S8).

Extrapolating our results to humans is complicated by fundamental differences in bile salt synthesis between mice and man. While hydrophobic chenodeoxycholate is rapidly converted to hydrophilic muricholates in the livers of mice, this additional hydroxylation reaction does not occur in humans. Therefore, FXR activation is likely to result in a more hydrophobic bile salt pool in humans, which would in theory lead to decreased FNS excretion and TICE.

In conclusion, this is the first study to demonstrate that the intestine is capable of eliminating very large quantities of cholesterol from the body via a direct blood-borne pathway. The flux of cholesterol through the TICE pathway is regulated by an interplay between the cholesterol exporter ABCG5/G8 and bile salts within the intestinal lumen. In particular, the physical-chemical properties of those luminal bile salts appear to play a major role in governing body cholesterol fluxes by impacting on ABCG5/G8 activity. The current study provides a strong rationale for the consideration of combination therapies including hydrophilic bile salts for the management of lipid disorders and protection of atherosclerosis and cardiovascular disease.

Figure legends

FIGURE 1. Effect of PX20606 on plasma lipids and sterol excretion in wild-type mice

C57BL/6J mice were treated with 10 mg/kg/day PX20606 (PX), when indicated combined with the cholesterol absorption inhibitor ezetimibe (EZE), for 2 wks. (A) Plasma cholesterol and (B) triglycerides levels were measured. (C) Fecal bile salt and (D) neutral sterol excretion were assessed using gas chromatography. (E) Fractional cholesterol absorption was determined using the appearance of stably labeled cholesterol-D_5 (i.v.) and cholesterol-D_7 (oral) in plasma. (F) Fecal neutral sterol excretion during first 8 days of PX treatment measured by gas chromatography. * $p<0.05$ vs. control treated (CTRL) animals, # $p<0.05$ vs. ezetimibe-treated animals, and $ $p<0.05$ vs. PX-treated animals (n=7 mice/group).

FIGURE 2. Sterol fluxes in PX20606-treated mice.

C57BL/6J mice were treated with 10 mg/kg/day PX20606 (PX), when indicated combined with the cholesterol absorption inhibitor ezetimibe (EZE), for 2 wks. At the end of the experiment (A) Bile flow, (B) biliary bile salt and (C) biliary cholesterol secretion were determined. (D) Transintestinal cholesterol excretion (TICE) was calculated according to the formula $TICE=FNS-((Chol_{diet}+Chol_{bile})*(1-Fa))$, where FNS means fecal neutral sterols and Fa is fractional cholesterol absorption. (E) Kinetics of intravenously administered cholesterol-D_5 label as measured by gas chromatography mass-spectrometry (GC-MS). (F) Fecal excretion of intravenously injected cholesterol-D_5 label calculated by multiplying the enrichment of cholesterol-D_5 label in feces with mass neutral sterol excretion. * $p < 0.05$ vs. control treated (CTRL) animals, # $p<0.05$ vs. ezetimibe-treated animals, and $ $p<0.05$ vs. PX-treated animals (n=7 mice/group).

FIGURE 3: PX20606-induced cholesterol excretion requires intestinal FXR.

Intestine-specific FXR-deficient (iFXR KO) mice and wild-type (WT) littermates were treated with 10 mg/kg/day PX20606 (PX), for 2 wks. (A) Fecal neutral sterol excretion determined by gas chromatography. (B) Transintestinal cholesterol excretion (TICE). (C) Fractional cholesterol absorption determined by dual cholesterol label administration. * $p<0.05$ vs. control-treated (CTRL) wild-type littermates, § $p<0.05$ vs. wild-type littermates with the same treatment (n=7 mice/group).

FIGURE 4. Reintroduction of intestinal FXR expression in total body FXR-deficient mice restores PX20606-induced transintestinal cholesterol excretion

Total body FXR-KO mice and intestine-specific FXR transgenic (FXR TG) mice were treated with 10 mg/kg/day PX20606 (PX) for 2 weeks. (A) Plasma cholesterol and (B) plasma triglyceride levels in FXR-KO and iFXR-TG mice, measured using commercially available reagents. (C) Fecal neutral sterol excretion in FXR-KO and iFXR-TG mice in response to PX treatment determined by gas chromatography. (D) Transintestinal cholesterol excretion (TICE). (E) Fractional cholesterol absorption in FXR-KO and iFXR-TG mice determined by dual cholesterol label administration. (F) Fecal bile salt excretion measured by gas chromatography. * $p<0.05$ vs. control-treated (CTRL) FXR-KO littermates, § $p<0.05$ vs. FXR-KO littermates with the same treatment (n=6-9 mice/group).

FIGURE 5. Effect of PX20606 and ezetimibe on cholesterol fluxes ABCG8 knock-out mice

ABCG8-deficient mice and wild-type (WT) littermates were treated with 10 mg/kg/day PX20606 (PX) either or not in combination with the cholesterol absorption inhibitor ezetimibe (EZE), for 2 wks. Mice

were infected with an ABCG8-encoding (AdABCG8) or control (AdNull) adenovirus as indicated (B-E right panels). (A) Hepatic and intestinal mRNA expression of *Abcg5* and *Abcg8* (left panel) and ABCG5 protein expression on brush border membranes isolated from proximal intestinal enterocytes (right panel). (B) Fecal neutral sterols determined by gas chromatography. (C) Transintestinal cholesterol excretion (TICE). (D) Biliary cholesterol secretion and (E) plasma cholesterol levels measured by gas chromatography. * $p<0.05$ vs. Control (CTRL) treated mice of same genotype; # $p<0.05$ vs. EZE treated mice of same genotype; $ $p<0.05$ vs. PX treated mice of same genotype; § $p<0.05$ vs. wild-type or vs. AdNull-injected ABCG8 KO with the same treatment (n=3-7 animals per group). ABCG5/G8, ATP binding cassette subfamily G member 5/8.

Figure 6. FGF15/19 mediates fecal neutral sterol excretion

Intestine-specific FXR-deficient (iFXR KO) mice and wild-type (WT) littermates were treated with 10 mg/kg/day PX20606 (PX), for 2 wks. When indicated, mice were treated with fibroblast growth factor 19 (FGF19; 1 µg/kg/day, i.p.) during the last 8 days of the experiment. (A) Cholesterol synthesis C57BL/6J mice upon PX and PX/ezetimibe (EZE) treatment, determined using the stably labeled precursor [^{13}C]acetate. (B) Fecal neutral sterols in iFXR KO mice and WT littermates measured by gas chromatography. (C) Gene expression of *Cyp7a1* and *Cyp8b1* in iFXR-KO mice and WT littermates. (D) Biliary bile salt species distribution in iFXR-KO mice and WT littermates determined by gas chromatography. (E) Correlation between Heuman's hydrophobicity index of biliary bile salts and fecal neutral sterol excretion in iFXR-KO mice and WT littermates. (F) Biliary bile salt species distribution in ABCG8-KO mice, determined as for (D). Parameters from panel A were analyzed in n=7 mice/group. Parameters from panels B-F were analyzed in n=3-7 mice/group. * $p < 0.05$ vs. Control (CTRL) of same genotype; # $p<0.05$ vs. EZE of same genotype; $ $p<0.05$ vs. PX of same genotype; § $p < 0.05$ vs. same

treatment different genotype; + $p < 0.05$ vs control-treated with FGF19. α-MCA, α-muricholic acid; β-MCA, β-muricholic acid; CA, cholic acid; CDCA, chenodeoxycholic acid; CYP7A1, cytochrome P450 family 7 subfamily A member 1; CYP8B1, cytochrome P450 family 8 subfamily B member 1; DCA, deoxycholic acid; HDCA, hyodeoxycholic acid; LCA, lithocholic acid; ω-MCA, ω-muricholic acid; UDCA, ursodeoxycholic acid.

FIGURE 7. PX20606-induced fecal neutral sterol excretion is mediated via bile

Bile duct diversion and model bile infusion was carried out in rats treated with 10 mg/kg/day PX20606 (PX) for two weeks and controls (CTRL) as detailed in the Methods section. Measurements of neutral sterol excretion were performed before and up three days after bile diversion/model bile infusion. (A) Biliary bile salt species distribution in PX-treated rats before infusion of model bile determined by gas chromatography. (B) Fecal Neutral Sterol excretion before ('Endogenous bile') and after bile duct diversion/model bile infusion. (C) Hepatic mRNA expression of *Cyp7a1, Cyp8b1* and *Shp* as well as ileal *Fgf19* mRNA expression after three days of model bile infusion. * $p < 0.05$ vs. CTRL; $ $p < 0.05$ vs. PX-treated rats before bile diversion (n=3-6 rats/group). CYP7A1, cytochrome P450 family 7 subfamily A member 1; CYP8B1, cytochrome P450 family 8 subfamily B member 1; SHP, small heterodimer partner.

REFERENCES

1. Dietschy JM, Turley SD, Spady DK. Role of liver in the maintenance of cholesterol and low density lipoprotein homeostasis in different animal species, including humans. J Lipid Res 1993;34:1637-1659.

2. Brufau G, Groen AK, Kuipers F. Reverse cholesterol transport revisited: contribution of biliary versus intestinal cholesterol excretion. Arterioscler Thromb Vasc Biol 2011;31:1726-1733.

3. **Temel RE**, **Brown JM**. A new model of reverse cholesterol transport: enTICEing strategies to stimulate intestinal cholesterol excretion. Trends Pharmacol Sci 2015;36:440-451.

4. **van der Veen JN**, **van Dijk TH**, Vrins CL, et al. Activation of the liver X receptor stimulates trans-intestinal excretion of plasma cholesterol. J Biol Chem 2009;284:19211-19219.

5. **Le May C**, **Berger JM**, Lespine A, et al. Transintestinal cholesterol excretion is an active metabolic process modulated by PCSK9 and statin involving ABCB1. Arterioscler Thromb Vasc Biol 2013;33:1484-1493.

6. Temel RE, Sawyer JK, Yu L, et al. Biliary sterol secretion is not required for macrophage reverse cholesterol transport. Cell Metab 2010;12:96-102.

7. **van der Velde AE**, **Vrins CL**, van den Oever K, et al. Direct intestinal cholesterol secretion contributes significantly to total fecal neutral sterol excretion in mice. Gastroenterology 2007;133:967-975.

8. van der Velde AE, Vrins CL, van den Oever K, et al. Regulation of direct transintestinal cholesterol excretion in mice. Am J Physiol Gastrointest Liver Physiol 2008;295:G203-G208.

9. Brufau G, Kuipers F, Lin Y, et al. A reappraisal of the mechanism by which plant sterols promote neutral sterol loss in mice. PLoS One 2011;6:e21576.

10. Warrier M, Shih DM, Burrows AC, et al. The TMAO-Generating Enzyme Flavin Monooxygenase 3 Is a Central Regulator of Cholesterol Balance. Cell Rep 2015;.

11. Voshol PJ, Schwarz M, Rigotti A, et al. Down-regulation of intestinal scavenger receptor class B, type I (SR-BI) expression in rodents under conditions of deficient bile delivery to the intestine. Biochem J 2001;356:317-325.

12. Kuipers F, Bloks VW, Groen AK. Beyond intestinal soap--bile acids in metabolic control. Nat Rev Endocrinol 2014;10:488-498.

13. Li T, Chiang JY. Bile acid signaling in metabolic disease and drug therapy. Pharmacol Rev 2014;66:948-983.

14. **Makishima M**, **Okamoto AY**, **Repa JJ**, et al. Identification of a nuclear receptor for bile acids. Science 1999;284:1362-1365.

15. Parks DJ, Blanchard SG, Bledsoe RK, et al. Bile acids: natural ligands for an orphan nuclear receptor. Science 1999;284:1365-1368.

16. Wang H, Chen J, Hollister K, et al. Endogenous bile acids are ligands for the nuclear receptor FXR/BAR. Mol Cell 1999;3:543-553.

17. Inagaki T, Choi M, Moschetta A, et al. Fibroblast growth factor 15 functions as an enterohepatic signal to regulate bile acid homeostasis. Cell Metab 2005;2:217-225.

18. Madison BB, Dunbar L, Qiao XT, et al. Cis elements of the villin gene control expression in restricted domains of the vertical (crypt) and horizontal (duodenum, cecum) axes of the intestine. J Biol Chem 2002;277:33275-33283.

19. **Kok T**, **Hulzebos CV**, Wolters H, et al. Enterohepatic circulation of bile salts in farnesoid X receptor-deficient mice: efficient intestinal bile salt absorption in the absence of ileal bile acid-binding protein. J Biol Chem 2003;278:41930-41937.

20. Klett EL, Lu K, Kosters A, et al. A mouse model of sitosterolemia: absence of Abcg8/sterolin-2 results in failure to secrete biliary cholesterol. BMC Med 2004;2:5.

21. Abel U, Schluter T, Schulz A, et al. Synthesis and pharmacological validation of a novel series of non-steroidal FXR agonists. Bioorg Med Chem Lett 2010;20:4911-4917.

22. Hambruch E, Miyazaki-Anzai S, Hahn U, et al. Synthetic farnesoid X receptor agonists induce high-density lipoprotein-mediated transhepatic cholesterol efflux in mice and monkeys and prevent atherosclerosis in cholesteryl ester transfer protein transgenic low-density lipoprotein receptor (-/-) mice. J Pharmacol Exp Ther 2012;343:556-567.

23. Kuipers F, van Ree JM, Hofker MH, et al. Altered lipid metabolism in apolipoprotein E-deficient mice does not affect cholesterol balance across the liver. Hepatology 1996;24:241-247.

24. Kuipers F, Havinga R, Bosschieter H, et al. Enterohepatic circulation in the rat. Gastroenterology 1985;88:403-411.

25. Gamble W, Vaughan M, Kruth HS, et al. Procedure for determination of free and total cholesterol in micro- or nanogram amounts suitable for studies with cultured cells. J Lipid Res 1978;19:1068-1070.

26. Out C, Patankar JV, Doktorova M, et al. Gut microbiota inhibit Asbt-dependent intestinal bile acid reabsorption via Gata4. J Hepatol 2015;63:697-704.

27. Heuman DM. Quantitative estimation of the hydrophilic-hydrophobic balance of mixed bile salt solutions. J Lipid Res 1989;30:719-730.

28. Brufau G, Groen AK. Characterization of Whole Body Cholesterol Fluxes in the Mouse. Curr Protoc Mouse Biol 2011;1:413-427.

29. Schmitz J, Preiser H, Maestracci D, et al, Crane RK. Purification of the human intestinal brush border membrane. Biochim Biophys Acta 1973;323:98-112.

30. Kosters A, Frijters RJ, Schaap FG, et al. Relation between hepatic expression of ATP-binding cassette transporters G5 and G8 and biliary cholesterol secretion in mice. J Hepatol 2003;38:710-716.

31. Stricker D. BrightStat.com: free statistics online. Comput Methods Programs Biomed 2008;92:135-143.

32. Wang J, Zhang DW, Lei Y, et al. Purification and reconstitution of sterol transfer by native mouse ABCG5 and ABCG8. Biochemistry 2008;47:5194-5204.

33. Dietschy JM, Turley SD. Control of cholesterol turnover in the mouse. J Biol Chem 2002;277:3801-3804.

34. Jakulj L, Vissers MN, van Roomen CP, et al. Ezetimibe stimulates faecal neutral sterol excretion depending on abcg8 function in mice. FEBS Lett 2010;584:3625-3628.

35. Wang Y, Liu X, Pijut SS, et al. The combination of ezetimibe and ursodiol promotes fecal sterol excretion and reveals a G5G8-independent pathway for cholesterol elimination. J Lipid Res 2015;56:810-820.

36. Claudel T, Sturm E, Duez H, et al. Bile acid-activated nuclear receptor FXR suppresses apolipoprotein A-I transcription via a negative FXR response element. J Clin Invest 2002;109:961-971.

37. Zhang Y, Yin L, Anderson J, et al. Identification of novel pathways that control farnesoid X receptor-mediated hypocholesterolemia. J Biol Chem 2010;285:3035-3043.

38. **Fu T**, **Kim YC**, Byun S, et al. FXR primes the liver for intestinal FGF15 signaling by transient induction of betaKlotho. Mol Endocrinol 2015;me20151226.

39. Kir S, Beddow SA, Samuel VT, et al. FGF19 as a postprandial, insulin-independent activator of hepatic protein and glycogen synthesis. Science 2011;331:1621-1624.

40. Kliewer SA, Mangelsdorf DJ. Bile Acids as Hormones: The FXR-FGF15/19 Pathway. Dig Dis 2015;33:327-331.

41. Vrins C, Vink E, Vandenberghe KE, et al. The sterol transporting heterodimer ABCG5/ABCG8 requires bile salts to mediate cholesterol efflux. FEBS Lett 2007;581:4616-4620.

Author names in bold designate shared co-first authorship

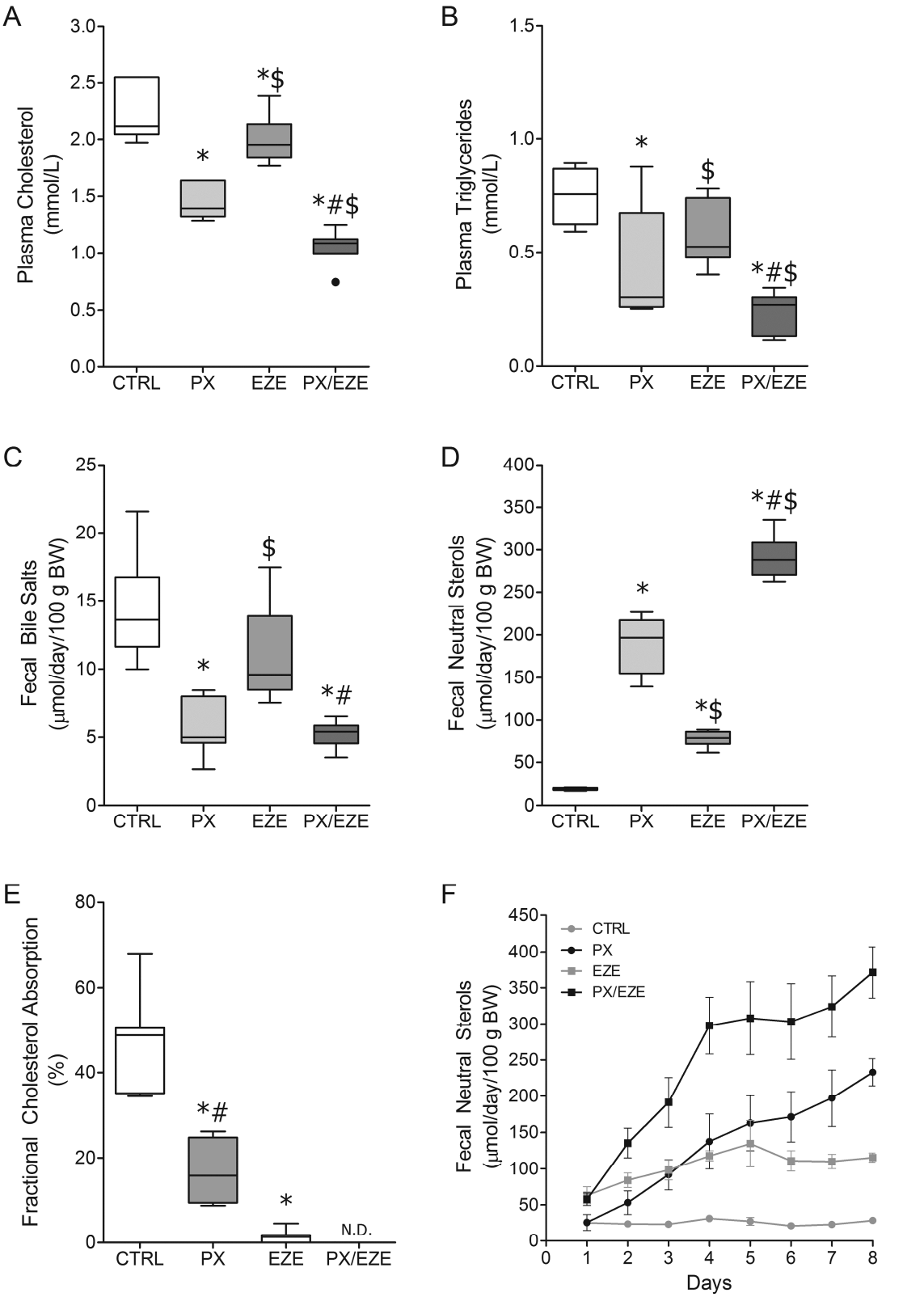
A
Plasma Cholesterol (mmol/L)
3.0
2.5
2.0
1.5
1.0
0.5
0.0
*
*$
*#$
CTRL
PX
EZE
PX/EZE
B
Plasma Triglycerides (mmol/L)
1.5
1.0
0.5
0.0
*
$
*#$
CTRL
PX
EZE
PX/EZE
C
Fecal Bile Salts (µmol/day/100 g BW)
25
20
15
10
5
0
*
$
*#
CTRL
PX
EZE
PX/EZE
D
Fecal Neutral Sterols (µmol/day/100 g BW)
400
350
300
250
200
150
100
50
0
*
*$
*#$
CTRL
PX
EZE
PX/EZE
E
Fractional Cholesterol Absorption (%)
80
60
40
20
0
*#
*
N.D.
CTRL
PX
EZE
PX/EZE
F
Fecal Neutral Sterols (µmol/day/100 g BW)
450
400
350
300
250
200
150
100
50
0
CTRL
PX
EZE
PX/EZE
0
1
2
3
4
5
6
7
8
Days

Figure 1

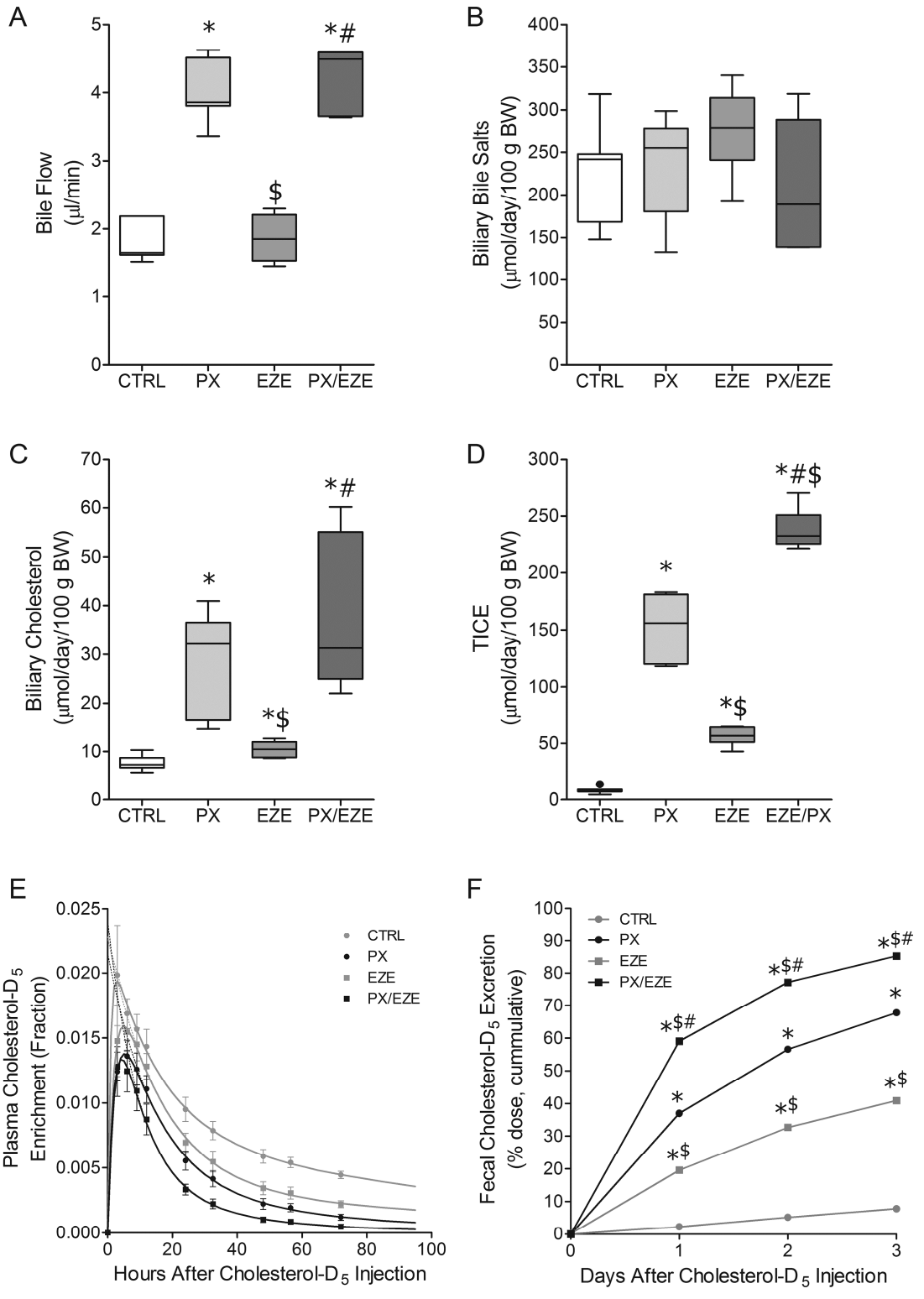
A
Bile Flow (µl/min)
CTRL
PX
EZE
PX/EZE
B
Biliary Bile Salts (µmol/day/100 g BW)
C
Biliary Cholesterol (µmol/day/100 g BW)
D
TICE (µmol/day/100 g BW)
EZE/PX
E
Plasma Cholesterol-D5 Enrichment (Fraction)
Hours After Cholesterol-D5 Injection
F
Fecal Cholesterol-D5 Excretion (% dose, cummulative)
Days After Cholesterol-D5 Injection

Figure 2

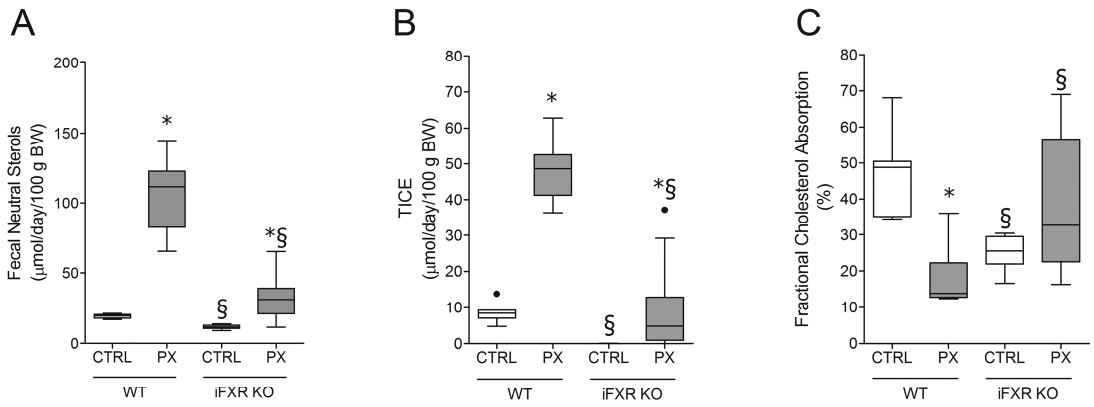

Figure 3

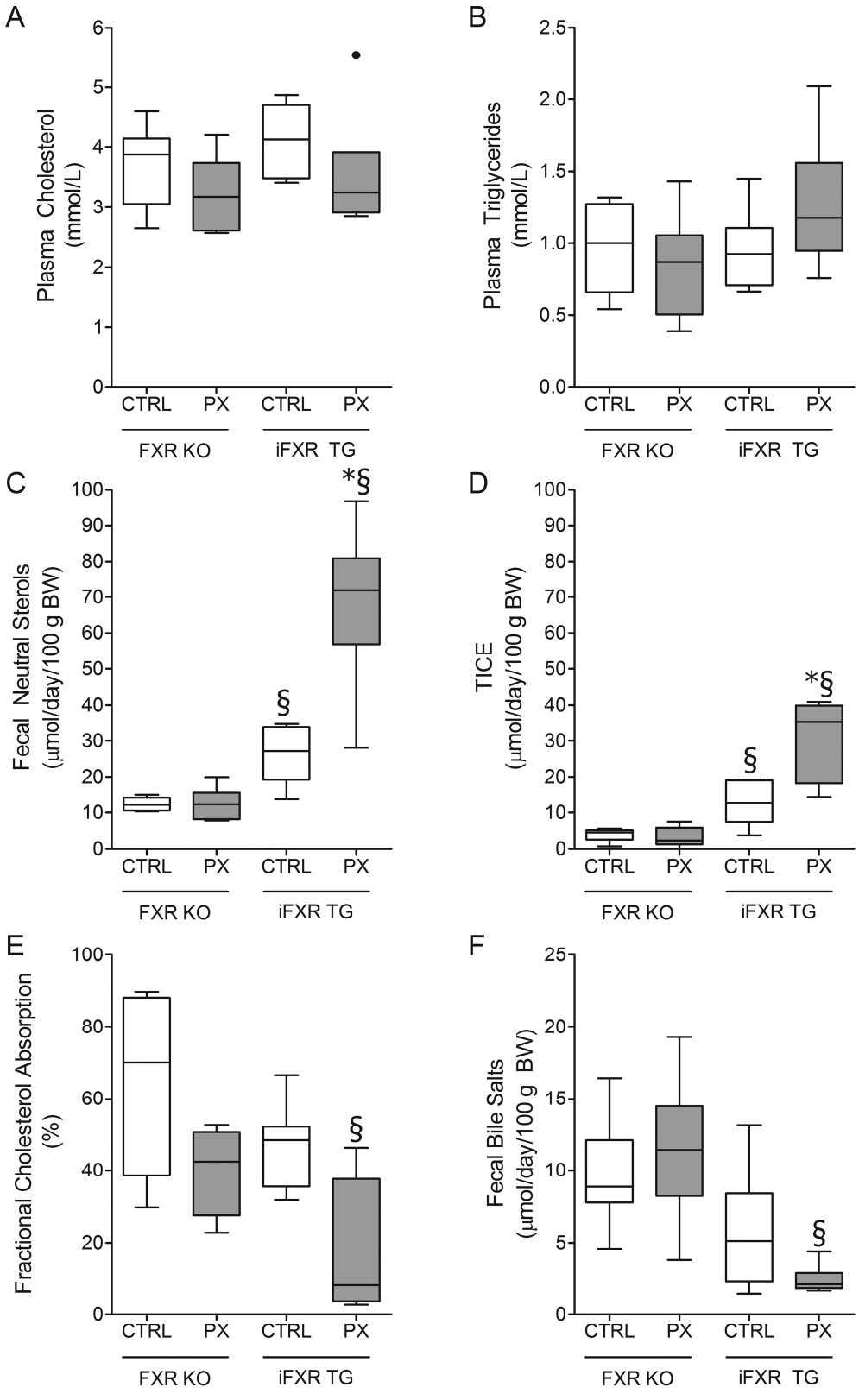
A
Plasma Cholesterol (mmol/L)
B
Plasma Triglycerides (mmol/L)
C
Fecal Neutral Sterols (µmol/day/100 g BW)
D
TICE (µmol/day/100 g BW)
E
Fractional Cholesterol Absorption (%)
F
Fecal Bile Salts (µmol/day/100 g BW)
CTRL
PX
FXR KO
iFXR TG
*§
§

Figure 4

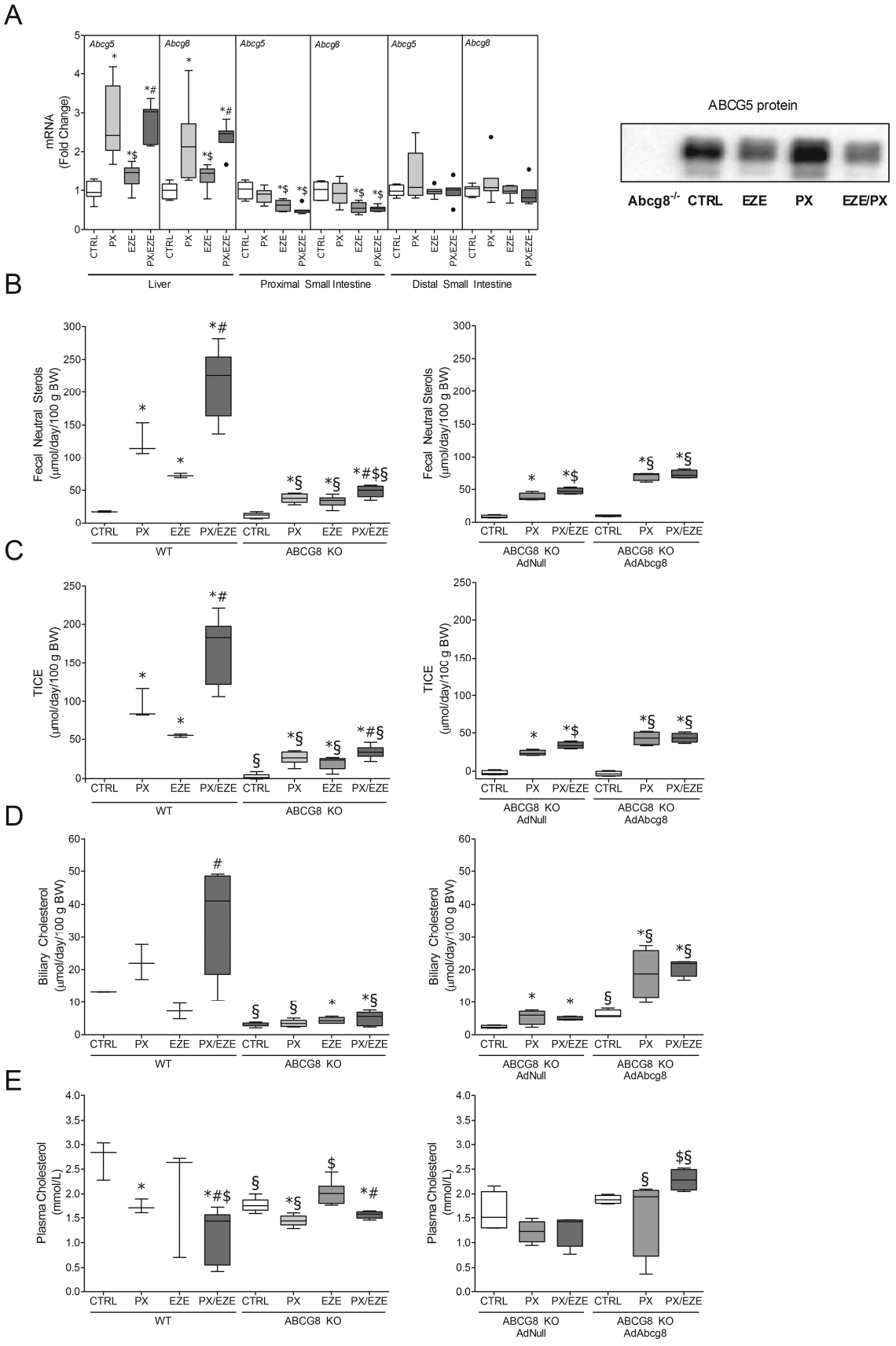
A
Abcg5
Abcg8
mRNA (Fold Change)
CTRL PX EZE PX/EZE
Liver
Proximal Small Intestine
Distal Small Intestine
ABCG5 protein
Abcg8-/- CTRL EZE PX EZE/PX
B
Fecal Neutral Sterols (µmol/day/100 g BW)
WT
ABCG8 KO
ABCG8 KO AdNull
ABCG8 KO AdAbcg8
C
TICE (µmol/day/100 g BW)
D
Biliary Cholesterol (µmol/day/100 g BW)
E
Plasma Cholesterol (mmol/L)

Figure 5

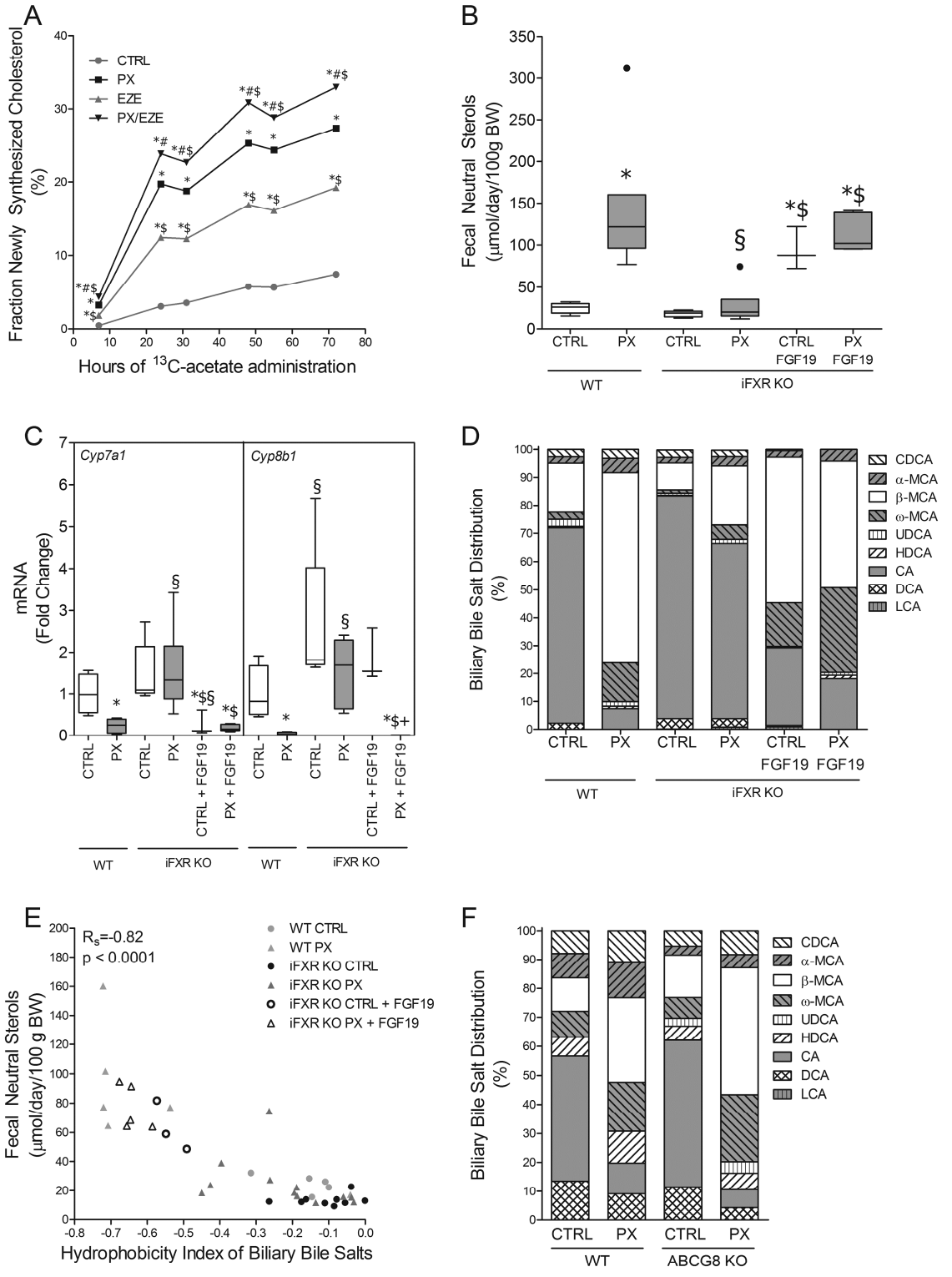
A
Fraction Newly Synthesized Cholesterol (%)
CTRL
PX
EZE
PX/EZE
Hours of 13C-acetate administration
B
Fecal Neutral Sterols (µmol/day/100g BW)
CTRL
PX
CTRL
PX
CTRL FGF19
PX FGF19
WT
iFXR KO
C
Cyp7a1
Cyp8b1
mRNA (Fold Change)
CTRL
PX
CTRL + FGF19
PX + FGF19
WT
iFXR KO
D
Biliary Bile Salt Distribution (%)
CDCA
α-MCA
β-MCA
ω-MCA
UDCA
HDCA
CA
DCA
LCA
CTRL FGF19
PX FGF19
E
Rs=-0.82
p < 0.0001
WT CTRL
WT PX
iFXR KO CTRL
iFXR KO PX
iFXR KO CTRL + FGF19
iFXR KO PX + FGF19
Fecal Neutral Sterols (µmol/day/100 g BW)
Hydrophobicity Index of Biliary Bile Salts
F
Biliary Bile Salt Distribution (%)
ABCG8 KO

Figure 6

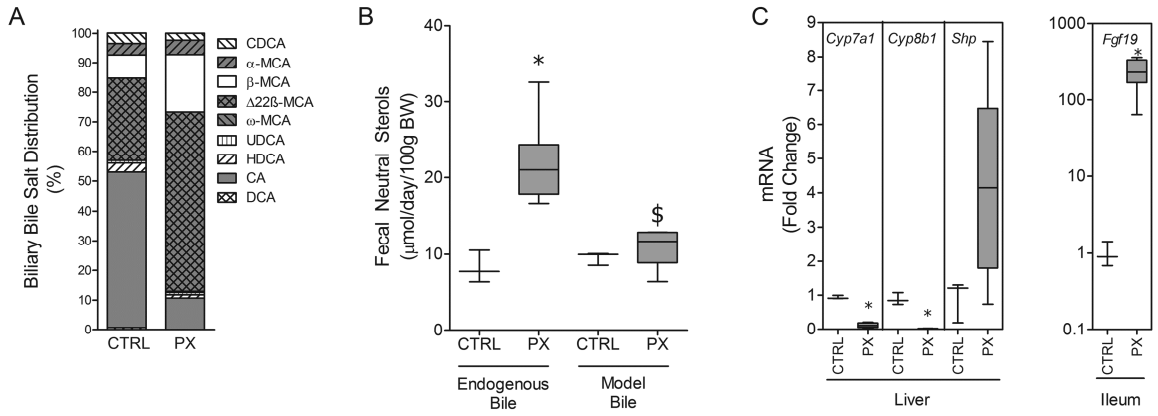

Figure 7

Supplementary Data and methods

Intestinal FXR Controls Transintestinal Cholesterol Excretion in Mice

Jan Freark de Boer, Marleen Schonewille, Marije Boesjes, Henk Wolters, Vincent W. Bloks, Trijnie Bos, Theo H. van Dijk, Angelika Jurdzinski, Renze Boverhof, Justina C. Wolters, Jan A. Kuivenhoven, Jan M. van Deursen, Ronald P.J. Oude Elferink, Antonio Moschetta, Claus Kremoser,Henkjan J. Verkade, Folkert Kuipers, Albert K. Groen

Supplementary Figures: 8

Supplementary Experimental Procedures

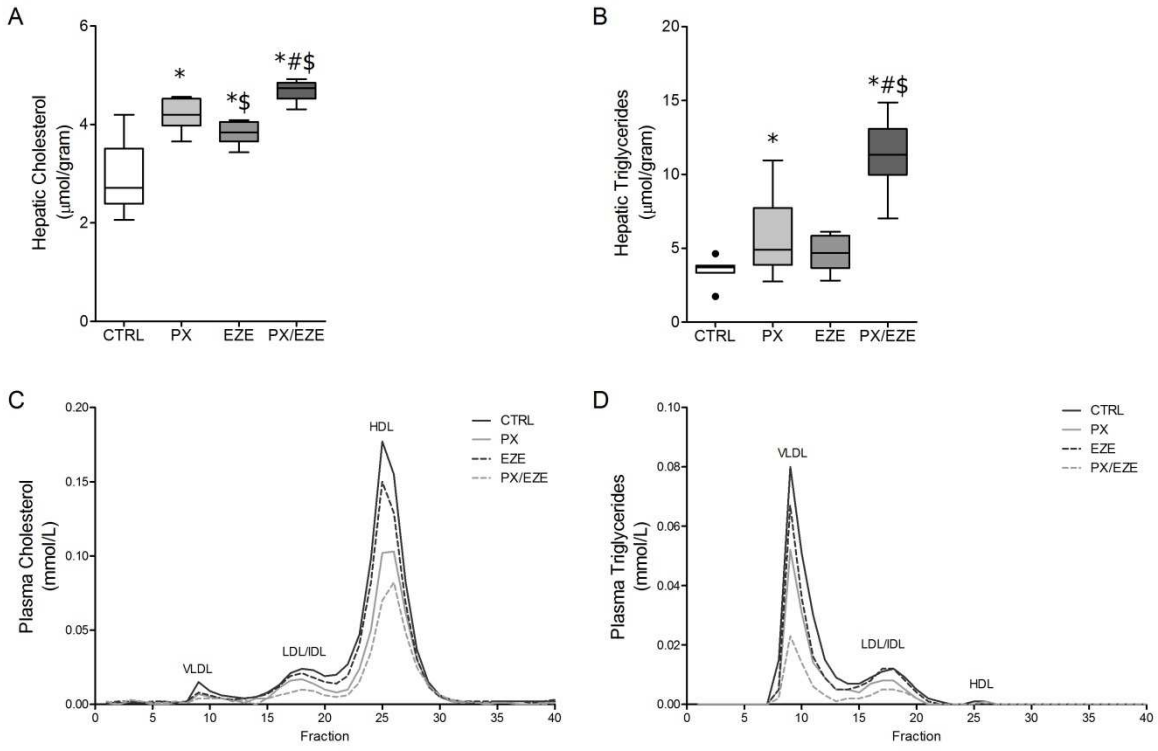

Figure S1: Hepatic lipids and plasma lipoprotein distribution upon FXR activation with PX20606

(A) Hepatic cholesterol levels in control (CTRL) mice and mice treated with PX20606 (PX), ezetimibe (EZE) or both compounds (PX/EZE). (B) Hepatic triglyceride levels in control mice or mice treated with PX, EZE or both compounds. (C) Cholesterol concentration in lipoprotein fractions after separation of pooled plasma samples (n=7 animals per group) by fast protein liquid chromatography (FPLC). (D) Triglyceride concentration in lipoprotein fractions after separation of pooled plasma samples (n=7 animals per group) by FPLC. * $p < 0.05$ vs. CTRL, \$ $p < 0.05$ vs. PX, # $p < 0.05$ vs. EZE. HDL, high-density lipoprotein; LDL, low-density lipoprotein; VLDL, very low-density lipoprotein.

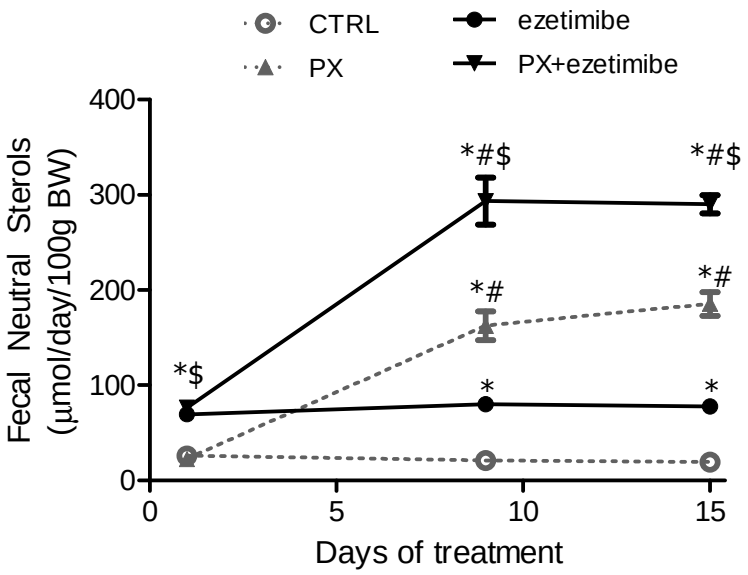

Figure S2: Alterations of fecal neutral sterol secretion upon treatment with PX20606, ezetimibe or both compounds during the 15-day treatment period

Fecal neutral sterol excretion in C57BL-6J mice measured the first 24h after onset of treatment (feces collected on day 1) as well as after 9 and 15 days. Data are presented as mean ± SEM of 7 animals per group. * $p<0.05$ vs. control treated animals, $^{\#}$ $p<0.05$ vs. animals treated with ezetimibe only, $^{\$}$ $p<0.05$ vs. animals treated with PX only. CTRL, control; PX, PX20606.

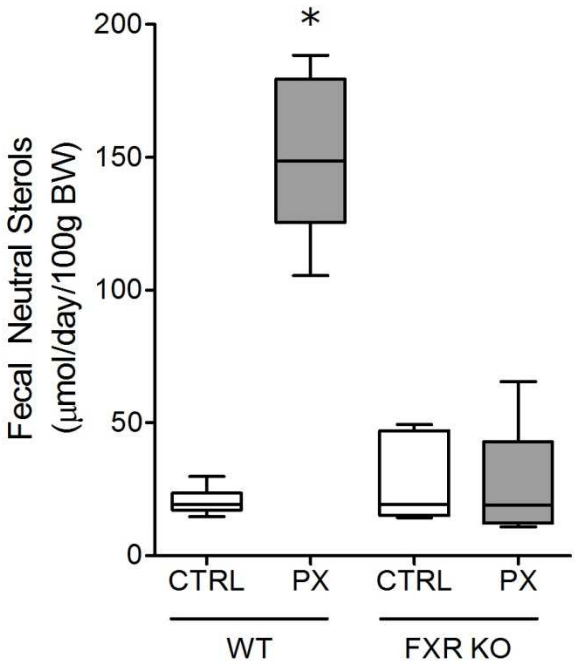

Figure S3: Fecal neutral sterols in FXR knock-out mice

Fecal neutral sterol excretion in wild-type and FXR KO mice after two weeks of treatment with or without PX20606 (PX). * $p<0.05$ vs. control treated animals. CTRL, control; PX, PX20606; WT, wild-type.

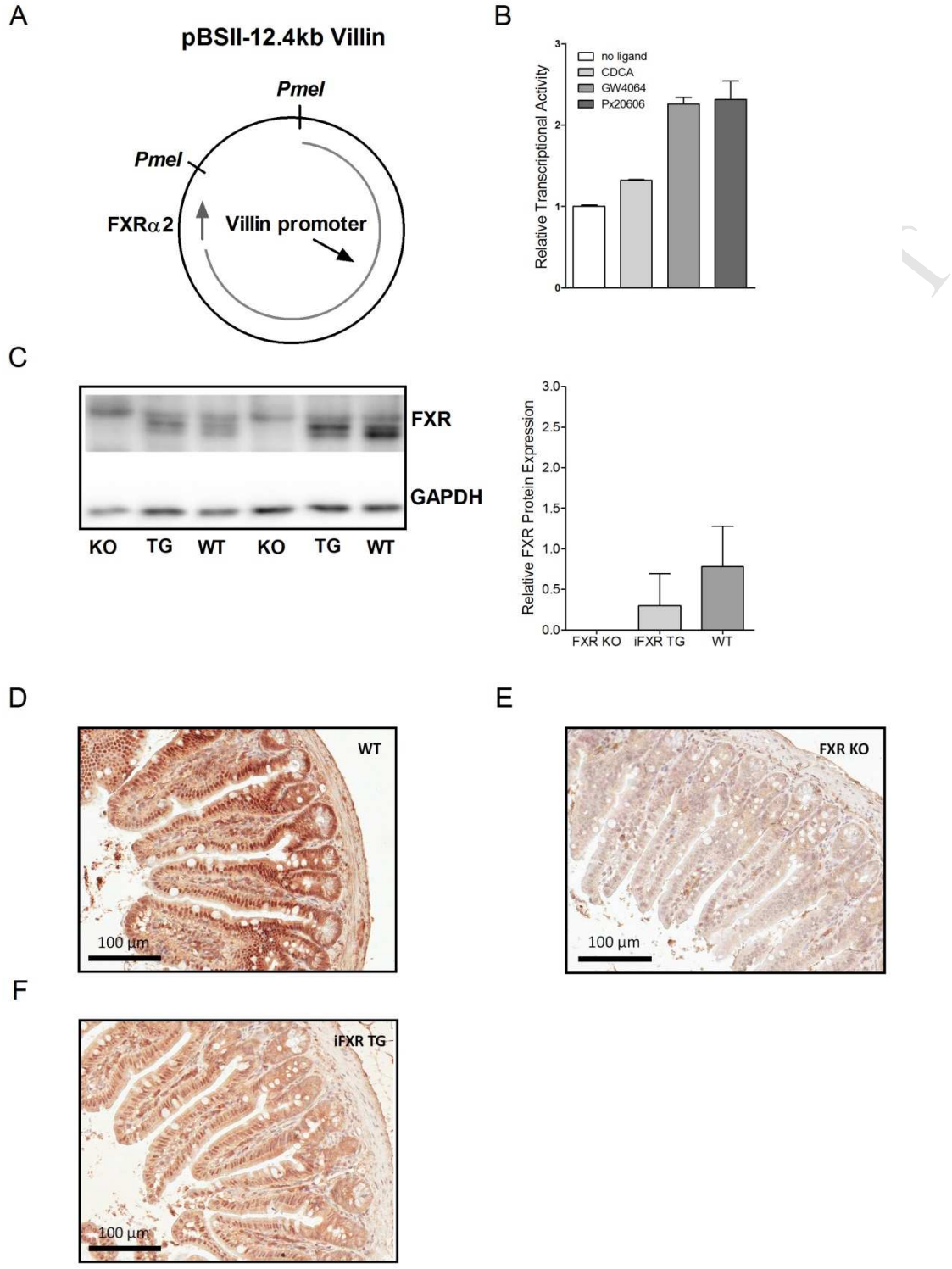

Figure S4: Generation of intestine-specific FXR transgenic mice

(A) Transgene construct of murine FXRα2. The mouse villin promoter was ligated to the murine *Fxrα2* gene. The construct was restricted from the backbone using *PmeI* and the resulting villin-FXRα2 fragment was quantified for microinjection. (B) Transcriptional activity of murine FXRα2 was tested in response to several FXR ligands. A luciferase assay was performed using an luciferase reporter containing tandem copies of FXRE from SHP and activity is shown in fold induction. (C) FXR protein expression levels were measured in mucosa of the distal ileum of chow-fed FXR KO, iFXR TG and WT mice. FXR protein levels were corrected for GAPDH protein levels. Data are presented as means ± SD (n=5 mice/group). (D) Immunohistochemistry staining using FXR antibody in the distal ileum of wildtype (E) FXR knockout and (F) iFXR transgenic mice.

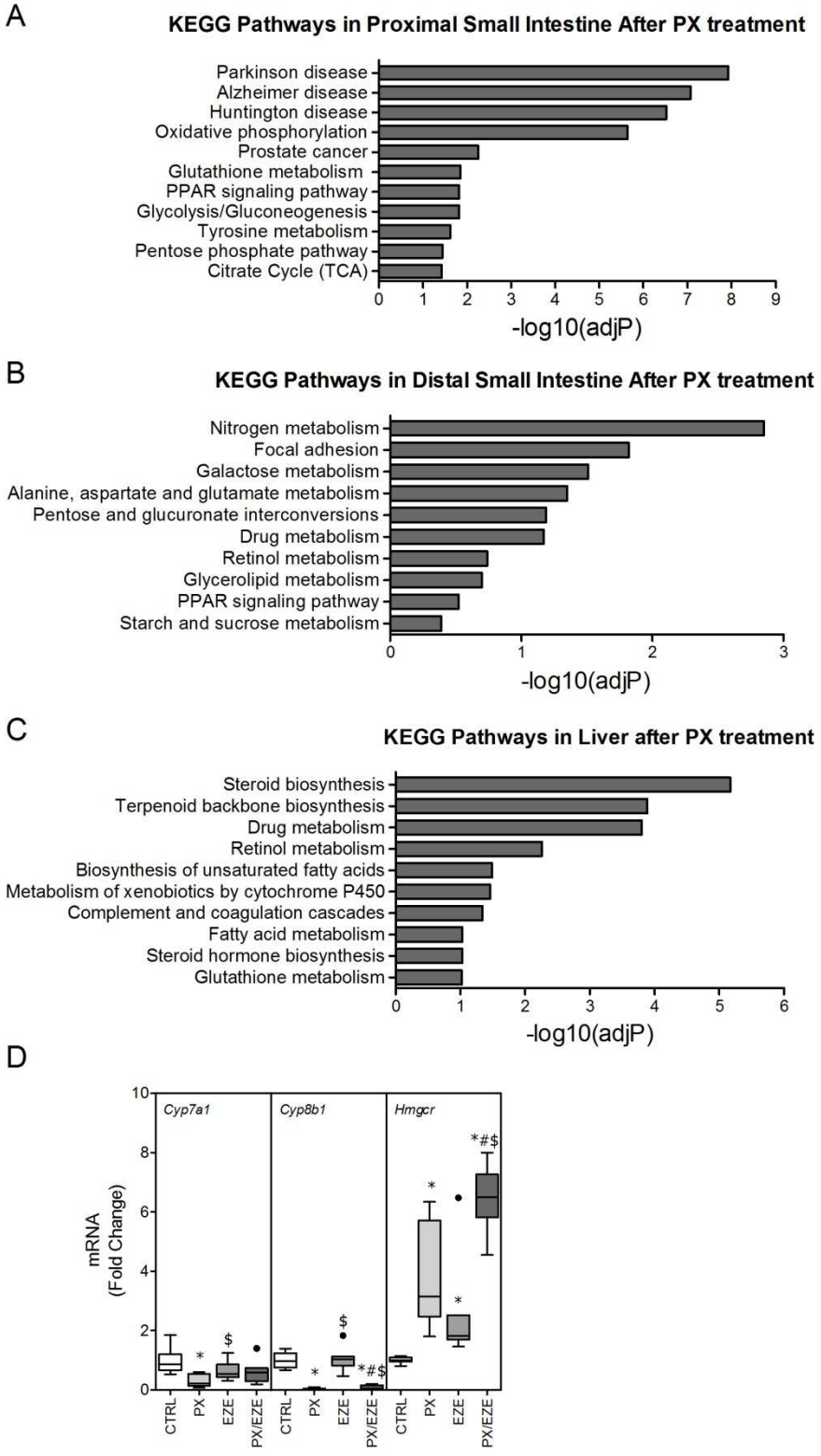

Figure S5: KEGG pathways analysis in liver, proximal and distal small intestine

KEGG pathway analyses of changes in mRNA expression in (A) proximal small intestine, (B) distal small intestine and (C) liver after 2 weeks of PX20606 (PX) treatment. (D) Hepatic mRNA expression of *Cyp7a1*, *Cyp8b1*, and *Hmgcr* after 2 weeks of treatment with PX or ezetimibe (EZE) determined by QPCR. * $p<0.05$ vs. control treated animals, $ $p<0.05$ vs. PX-treated animals, and # $p<0.05$ vs. ezetimibe-treated animals (n=7 mice/group). CTRL, Control; *Cyp7a1*, cytochrome P450 family 7 subfamily A member 1; *Cyp8b1*, cytochrome P450 family 8 subfamily B member 1; EZE, ezetimibe; KEGG, Kyoto encyclopedia of genes and genomes; *Hmgcr*, 3-hydroxy-3-methylglutaryl-CoA reductase; PX, PX20606.

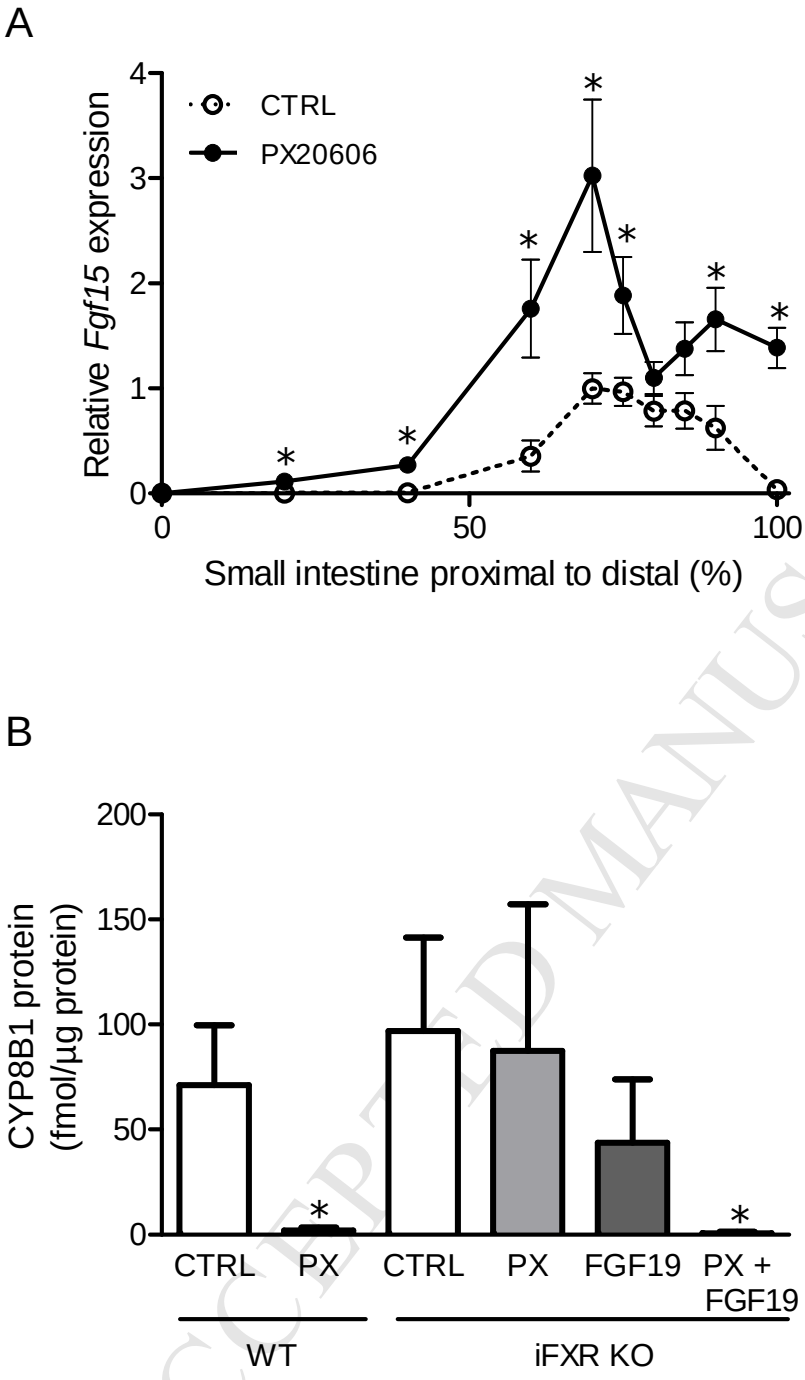

Figure S6: *Fgf15* mRNA expression in the small intestine in response to PX20606 and hepatic CYP8B1 protein expression in wild-type and intestine-specific FXR KO mice

(A) Expression of Fgf15 mRNA over the entire length of the small intestine in C57BL-6J mice and controls (n=7 animals/group). Expression levels were normalized to 36B4. Data are presented as means ± SEM. (B) CYP8B1 protein expression in livers of WT and intestine-specific FXR knock-out (iFXR KO) mice in response to PX as well as CYP8B1 expression in iFXR KO mice treated with FGF19 or PX/FGF19 (n=3-7 mice/group as mean + SD). * $p<0.05$ compared to control animals of the same genotype. CTRL, control; PX, PX20606.

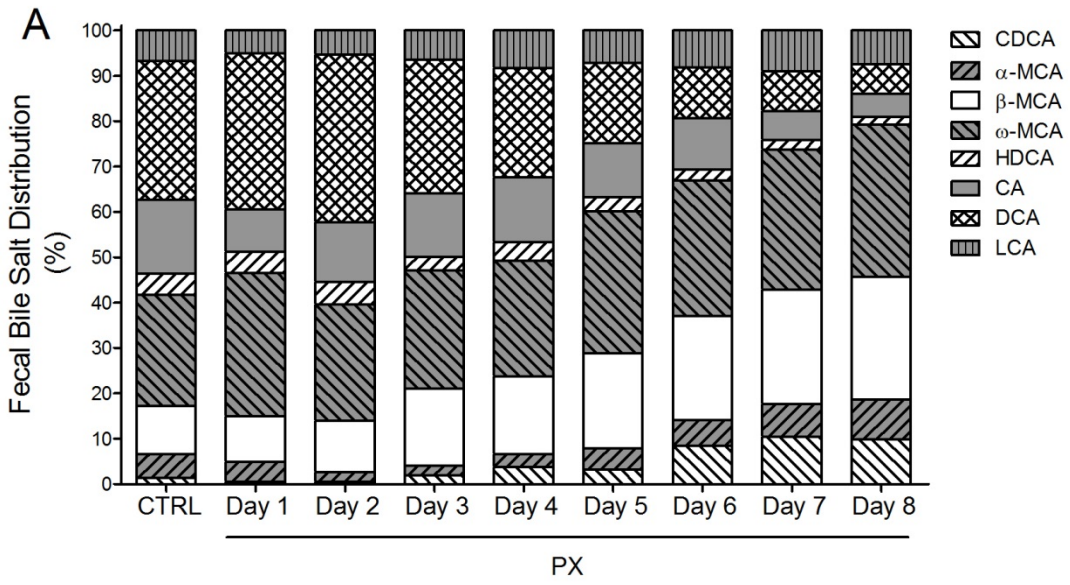

Figure S7: Change of bile salt species distribution in feces during 8 days of PX treatment

(A) Fecal bile salt species distribution during 8 days of treatment with PX20606 (n=7 mice/group). α-MCA, α-muricholic acid; β-MCA, β-muricholic acid; CA, cholic acid; CDCA, chenodeoxycholic acid; CTRL, control; DCA, deoxycholic acid; HDCA, hyodeoxycholic acid; LCA, lithocholic acid; PX, PX20606; ω-MCA, ω-muricholic acid.

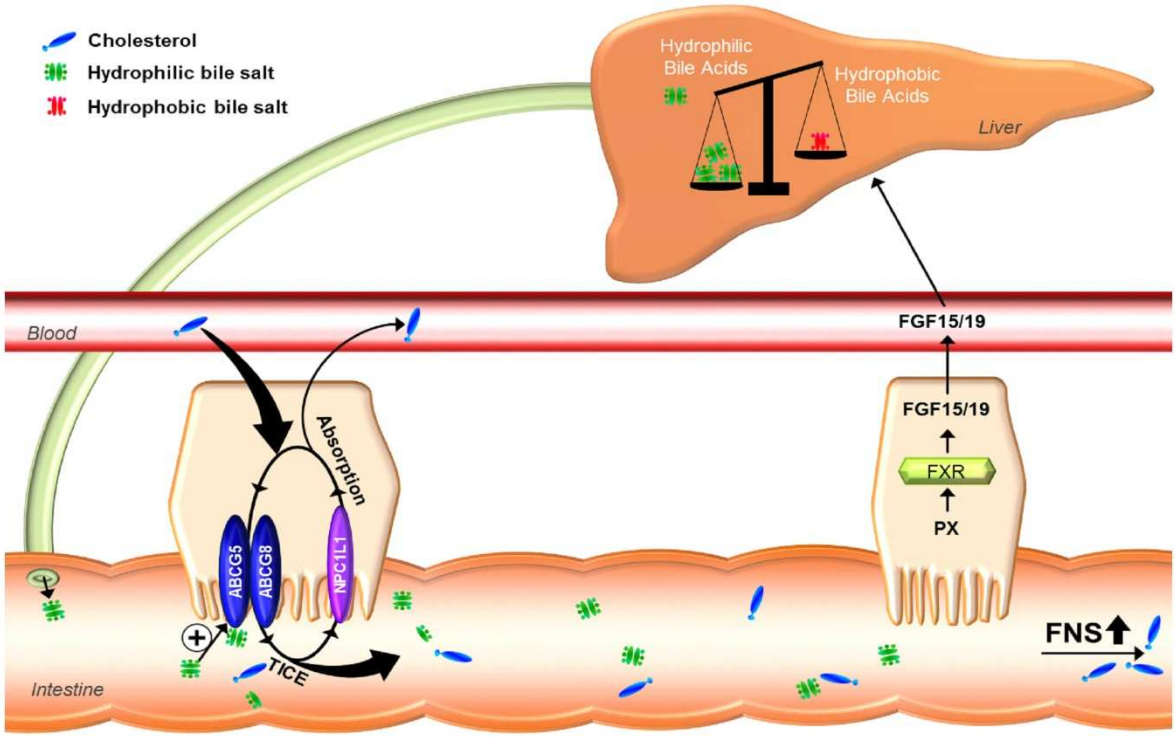

Figure S8: Graphical representation of the proposed mechanism driving the PX20606-induced increase in fecal neutral sterol (FNS) excretion and TICE.

PX20606 (PX) activates FXR in the intestine, leading to the production of FGF15/19 which, in turn, causes a shift in bile salt pool composition towards more hydrophilic bile salts. At the level of the enterocyte, excretion of cholesterol from the cell into the intestinal lumen is induced in a manner that largely depends on the activity of ABCG5/G8. As the amount of ABCG5/G8 protein on the brush border membrane remains unchanged upon PX-treatment, the transport activity must be increased. Hydrophilic bile salts may facilitate increased export of cholesterol from enterocytes by ABCG5/G8. When re-uptake of exported cholesterol is blocked by addition of ezetimibe to the diet of PX-treated mice, this leads to even further increased cholesterol disposal from the body.

Supplementary Experimental Procedures

Hepatic lipid extraction

Liver lipids were extracted from homogenates according to Bligh and Dyer.[1] Subsequently, hepatic cholesterol and triglyceride content was determined using commercially available reagents (DiaSys Diagnostic Systems, Holzheim, Germany and Roche Diagnostics, Mannheim, Germany).

Plasma lipoprotein separation

Separation of lipoproteins was performed using fast protein liquid chromatography (FPLC) applying a Superose-6 10/300 GL column (GE Healthcare, Uppsala, Sweden) as described previously.[2] Cholesterol and triglyceride concentrations in the individual fractions were determined using commercially available reagents (DiaSys Diagnostic Systems and Roche Diagnostics).

Plasmid construction and generation of intestine-specific FXRα2 mice

The coding sequences of murine FXRα2 was amplified using specific primer pairs (forward; TACTACGGATCCACCATGAATCTGATTGGGGACTCC, reverse; TACTACGCGGCCGCTCACTGCACAT CCCAGATCT) harboring a Kozak consensus ATG initiation codon and a *BamH1* restriction side at the 5' end and a *Not1* restriction side at the 3' end. As a template source, cDNA was synthesized from hepatic RNA from C57BL/6J mice. The products were cloned into pcDNA5/FRT/TO (Life Technologies, Bleiswijk, The Netherlands). The presence of the correct gene was sequence-verified. Subsequently, the MYTG insertion was deleted from FXRα1 using inverse PCR primers (forward; TTGTTAACTGAAATCCAGTG, reverse; ACATTCAGCCAACATCCCCA), to generate FXRα2. FXRα2 was cloned behind the villin promoter in the pBSII-12.4kbVillin plasmid[3] (kind gift from Deborah Gumucio, University of Michigan Medical School, Ann Arbor MI, USA). FXRα2 was restricted from pCDNA5/FRT/TO using *PmeI* and *XhoI* and was ligated into the 12.4 kbVillin plasmid restricted using *SmaI* and *XhoI*. The presence of the correct insert and orientation was sequence-verified. Subsequently, the vector backbone was deleted by restriction using *PmeI* in the 12.4 kbVillin plasmid. The linear Villin-FXRα2 sequence was heat-inactivated and purified using gel electrophoresis. Intestine-specific murine-FXRα2 transgenic mice were generated by microinjection of the construct into fertilized FVB/NHsd eggs. Clones with the highest murine FXR mRNA expression levels were recovered. Mice were backcrossed to whole body FXR-deficient mice[4], on a C57BL/6J background, generating a model with intestine-specific expression of FXRα2 on a whole-body FXR knock-out background.

Cell culture, transfections and reporter assays

CV1 cells (a kind gift from Ronald M. Evans, Salk Institute, San Diego, USA) were maintained in DMEM (Gibco, Breda, The Netherlands) supplemented with 10% FCS (Sigma Aldrich Chemie BV, Zwijndrecht, The Netherlands), 100 U/ml penicillin and 100 µg/ml streptomycin (Gibco, Breda, The Netherlands). Cultures were maintained at 37°C and 5% CO2 in a humidified incubator. Cells were transiently transfected using FuGENE 6 transfection reagent (Promega, Leiden, The Netherlands). Cell lysis and luciferase assay were performed using a dual luciferase reporter assay system (Promega, Leiden, The Netherlands). Briefly, the human PGL4-SHP (CHR16_M0432_R1 and CHR1_M0312_R1, Switchgear Genomics, Menlo Park, CA, USA) promoter reporter was transfected together with the pcDNA5/FRT/TO vector containing murine FXR and RXR alpha/NR2B1 for 48 hrs. Cells remained untreated or were treated with 50µM CDCA (Sigma-Aldrich), 1µM GW4064 (Sigma-Aldrich) or 1µM PX[5,6] (Phenex Pharmaceuticals, Heidelberg, Germany) 24 prior to cell lysis.

Intestinal immunohistochemical protein expression of FXR

Briefly, after fixation in formaldehyde, intestinal pieces were embedded in paraffin and cut into 4µm sections. For immunohistochemistry, sections were deparaffinized and rehydrated. Antigen-retrieval was done in 0.01 M citrate buffer pH 6 at 100°C for 20 min. Endogenous peroxidase activity was blocked by incubation for 30 min in 3% H_2O_2 in phosphate-buffered saline (PBS). Sections were blocked with 5% goat serum in PBS for 30 min. Immunostaining was performed overnight at 4°C using anti-FXR (Perseus Proteomics, Tokyo, Japan; PP-A9033A-00) 0.01 mg/ml in 2% normal goat serum/1% bovine serum albumin in PBS. Sections were washed in PBS followed by a 60 min incubation with polyclonal goat anti-mouse immunoglobulins/biotinylated (Dako, Denmark; 1/200 dilution), and subsequent by a 60 min incubation with streptavidin/HRP (Dako, Denmark; 1/200 dilution), both in PBS containing 1% normal goat serum. Visualization of the immune complexes was performed with diaminobenzidine, followed by hematoxylin counterstaining for 60 sec. Sections were dehydrated and mounted with Eukitt (Sigma-Aldrich, USA).

Western blotting for FXR protein expression

Intestinal mucosa was homogenized in buffer containing 50 mM Tris (pH 7.4), 300 mM sucrose, 10 mM EDTA, 10 mM DTT and protease inhibitors (Complete; Roche Diagnostics, Almere, The Netherlands). Protein was determined using BCA protein assay (Pierce Biotechnology, Rockford, IL, USA). Intestinal homogenates (25 µg protein) for detection of FXR were electrophoresed through 7% polyacrylamide gels and blotted on Hybond ECL membranes (Amersham, Little Chalfont, UK). Membranes were blocked in phosphate-buffered saline (pH 7.4) containing 0.1% Tween 20 and 4 % skim milk powder. Membranes were incubated with anti-FXR antibody (clone no. A9033A, Perseus Proteomics Inc., Tokyo, Japan). After washing, immunocomplexes were detected using horseradish peroxidase-conjugated goat anti-mouse IgG2a (Southern Biotech, Uithoorn, The Netherlands) and SuperSignal West Dura substrate (Thermo Scientific, Rockford, IL, USA).

Microarray Analyses

For microarray analyses, total hepatic and proximal and distal intestinal RNA was prepared from C57BL/6J mice (n =4-6 per group) receiving diet with or without supplementation of 10 mg/kg/day PX20606, using TRI-reagent (Sigma-Aldrich, St. Louis, MO, USA). RNA quality and concentration was assessed using a Biorad Experion Bioanalyzer. Starting with 200 ng of RNA, with an RNA Quality Indicator of at least 8, RNA was amplified and labeled using the Illumina TotalPrep RNA Amplification Kit (Applied Biosystems, Nieuwekerk a/d IJssel, The Netherlands). The WG-6 v2 expression arrays, containing 45281 transcripts (Illumina, San Diego, USA), were processed according to the manufactures protocol and slides were scanned immediately. Quality control, normalization (quantile), batch correction (Combat), and statistics (IBMT) were performed in MADMAX.[7] A list of significantly changed annotated genes between PX (n = 4) and WT (n = 4), including False Discovery Rates (FDR)-corrected p-values (5% or 10%) was generated. All microarray data reported are described in accordance with MIAME guidelines and are available in the GEO (GSE74101). Identification of overrepresented functional categories and enrichment analysis among responsive genes and their grouping into functionally related clusters was performed using the DAVID Functional Annotation Clustering tool[8] and GSEA.[9]
Reviewers link: http://www.ncbi.nlm.nih.gov/geo/query/acc.cgi?token=irsrayeohfcntqx&acc=GSE74101

Quantification of CYP8B1 protein expression

Targeted proteomics[10] was used to quantify CYP8B1 in homogenized liver tissue via the isotopically labeled peptide standard VVQEDYVLK, containing 13C-labeled lysine (PolyQuant GmbH, Germany). Briefly, homogenized tissues (50 µg protein) were mixed with 3.22 fmol of standard peptide per 1 µg of total protein. In-gel tryptic digestion (1:100 g/g sequencing grade modified trypsin V5111, Promega) was performed after reduction with 10 mM dithiothreitol and alkylation with 55 mM iodoacetamide proteins, followed by solid phase extraction (SPE C18-Aq 50 mg/1mL, Gracepure) for sample cleanup. The peptide was targeted and analyzed by a triple quadrupole mass spectrometer (MS) equipped with a nano-electrospray ion source (TSQ Vantage, Thermo Scientific). Chromatographic separation was performed by liquid chromatography on a nano-UHPLC system (Ultimate UHPLC focused, Dionex) using a nano column (Acclaim PepMap100 C18, 75 µmx500mm 2µm, 100 Å) with a linear gradient from 3-60 % v/v acetonitrile plus 0.1% v/v formic acid in 110 minutes at a flowrate of 200 nL/min. The MS traces were manually curated using the Skyline software[11] prior to integration of the peak areas for quantification. The concentration of the endogenous peptide was calculated from the known concentration of the standard and expressed in fmol/µg of total protein.

References

1. Bligh EG, Dyer WJ. A rapid method of total lipid extraction and purification. Can J Biochem Physiol 1959;37:911-917.

2. Voshol PJ, Schwarz M, Rigotti A, Krieger M, Groen AK, Kuipers F. Down-regulation of intestinal scavenger receptor class B, type I (SR-BI) expression in rodents under conditions of deficient bile delivery to the intestine. Biochem J 2001;356:317-325.

3. Madison BB, Dunbar L, Qiao XT, Braunstein K, Braunstein E, Gumucio DL. Cis elements of the villin gene control expression in restricted domains of the vertical (crypt) and horizontal (duodenum, cecum) axes of the intestine. J Biol Chem 2002;277:33275-33283.

4. Kok T, Hulzebos CV, Wolters H, et al. Enterohepatic circulation of bile salts in farnesoid X receptor-deficient mice: efficient intestinal bile salt absorption in the absence of ileal bile acid-binding protein. J Biol Chem 2003;278:41930-41937.

5. Abel U, Schluter T, Schulz A, et al. Synthesis and pharmacological validation of a novel series of non-steroidal FXR agonists. Bioorg Med Chem Lett 2010;20:4911-4917.

6. Hambruch E, Miyazaki-Anzai S, Hahn U, et al. Synthetic farnesoid X receptor agonists induce high-density lipoprotein-mediated transhepatic cholesterol efflux in mice and monkeys and prevent atherosclerosis in cholesteryl ester transfer protein transgenic low-density lipoprotein receptor (-/-) mice. J Pharmacol Exp Ther 2012;343:556-567.

7. Lin K, Kools H, de Groot PJ, et al. MADMAX - Management and analysis database for multiple ~omics experiments. J Integr Bioinform 2011;8:160-jib-2011-160.

8. Dennis G,Jr, Sherman BT, Hosack DA, et al. DAVID: Database for Annotation, Visualization, and Integrated Discovery. Genome Biol 2003;4:P3.

9. Subramanian A, Tamayo P, Mootha VK, et al. Gene set enrichment analysis: a knowledge-based approach for interpreting genome-wide expression profiles. Proc Natl Acad Sci U S A 2005;102:15545-15550.

10. Schonewille M, de Boer JF, Mele L, et al. Statins increase hepatic cholesterol synthesis and stimulate fecal cholesterol elimination in mice. J Lipid Res 57: 1455-1464.

11. MacLean B, Tomazela DM, Shulman N, et al. Skyline: an open source document editor for creating and analyzing targeted proteomics experiments, Bioinformatics 26 (2010) 966-968